



AWESOME

WATER-ECOSYSTEM-FOOD

WEF PLANNING PORTFOLIOS

April, 2023



This project is part of the PRIMA Programme supported by the European Union, having received funding from it under grant agreement No 1942



| | |
|--------------------------------------|--|
| Programme Call: | PRIMA Call 2019 Section 1 Farming RIA |
| Project Number: | 1942 |
| Project Title: | AWESOME |
| Partners: | POLIMI (Project Coordinator), AUEB, YVC, UH, AF, RWTH, FEEM |
| Work-Package: | WP4 |
| Deliverable #: | D4.3 |
| Deliverable Type: | Document |
| Contractual Date of Delivery: | 30 April 2023 |
| Actual Date of Delivery: | 28 April 2023 |
| Title of Document: | Efficient WEF planning portfolios |
| Author(s): | Veronica Piuri, Matteo Giuliani, Elena Matta, Guang Yang, George Papagiannis, Athanasios Yanncopoulous, Martina Sardo, Davide Danilo Chiarelli, Maria Cristina Rulli, Andrea Castelletti |
| Content of this report: | Report about the design of efficient WEF planning portfolios under current and future scenarios. |
| Availability: | This report is public. |

| Document revisions | | |
|---|--|---------------|
| <i>Author</i> | <i>Revision content</i> | <i>Date</i> |
| Matteo Giuliani, Elena Matta | V00 - Table of content | 2 March 2023 |
| Veronica Piuri | V01 - First draft of the report | 13 March 2023 |
| Veronica Piuri, Elena Matta, George Papagiannis, Athanasios Yanncopoulous, Martina Sardo, Davide Danilo Chiarelli | V02 - Second draft of the report | 20 March 2023 |
| Matteo Giuliani, Veronica Piuri | V03 – First complete version of the report | 24 March 2023 |
| Elena Matta, Veronica Piuri | V04 – Final draft after PRIMA evaluation | 20 March 2024 |

Table of Content

| | |
|---|----|
| Table of Content | 3 |
| LIST OF ACRONYMS | 4 |
| EXECUTIVE SUMMARY | 5 |
| 1. INTRODUCTION | 6 |
| 2. THE NILE RIVER BASIN | 7 |
| 3. MESO LEVEL DECISION-ANALYTIC FRAMEWORK | 8 |
| STRATEGIC MODEL FOR THE NILE RIVER BASIN | 9 |
| OPTIMIZATION ENGINE | 12 |
| 4. FUTURE SCENARIOS | 13 |
| 4.1 URBAN DEMAND | 14 |
| 4.2 IRRIGATION DEMAND SCENARIOS | 15 |
| 4.3 STREAMFLOW PROJECTIONS | 17 |
| 3.3.1 Hydrologic modelling | 17 |
| 3.3.2 Climate scenarios | 21 |
| 5. RESULTS | 23 |
| 5.1 HISTORICAL CONDITIONS | 23 |
| 5.2 THE ROLE OF INTERNATIONAL COOPERATION | 33 |
| 5.3 FUTURE CONDITIONS | 34 |
| 6. CONCLUDING REMARKS | 44 |
| 7. REFERENCES | 46 |

LIST OF ACRONYMS

Abbreviations

| | |
|---------|--|
| ANN: | Artificial Neural Network |
| CAPEX: | Capital Expenditure |
| CHIRPS: | Climate Hazards Group InfraRed Precipitation with Station data |
| CHIRTS: | Climate Hazards Centre Infrared Temperature with Stations |
| D: | Deliverable |
| DAF: | Decision-Analytic Framework |
| DP: | Dynamic Programming |
| DPS: | Direct Policy Search |
| EMODPS: | Evolutionary Multi-Objective Direct Policy Search |
| ENTRO: | Eastern Nile Technical Regional Office |
| GCM: | General Circulation Model |
| GERD: | Grand Ethiopian Renaissance Dam |
| HAD: | High Aswan Dam |
| HBV: | Hydrologiska Byrans Vattenbalansavdelning |
| IPCC: | Intergovernmental Panel on Climate Change |
| MER: | Merowe dam |
| MOEA: | Multi-Objective Evolutionary Optimization Algorithms |
| NBR: | Nile River Basin |
| NSE: | Nash Sutcliffe Efficiency |
| OPEX: | Operational Expenditure |
| RBF: | Radial Basis Function |
| RCM: | Regional Climate Models |
| RCP: | Representative Concentrated Pathway |
| RMSE: | Root Mean Square Error |
| SDG: | Sustainable Development Goal |
| SDP: | Stochastic Dynamic Programming |
| SH: | Stakeholder |
| SSP: | Shared Socioeconomic Pathway |
| T: | Task |
| WEF: | Water Energy Food |
| WEFE: | Water Energy Food Environment |
| WP: | Work Package |

EXECUTIVE SUMMARY

Deliverable 4.3 describes the multi-objective design approach adopted for planning efficient portfolios under current and future scenarios. It summarizes the architecture of the meso-level Decision Analytic Framework and the future scenarios considered. The document includes the analysis of the results obtained by exploring synergies and tradeoffs across the Water, Energy, Food and Ecosystem Nexus components as quantified by the evaluation indicators formulated in D4.1. Our results show that the Nile River Basin features both strong tradeoffs and synergies across riparian countries, with the irrigation supply in Sudan playing a major role in allocating water between competing sectors. The future projections show a decrease of up to 20% of the Nile River's runoff and an increasing municipal demand in Egypt that lead to exacerbating tensions between the three countries. Notably, the potential reduction of the Egyptian water demand through different combinations of aquaponics, desalination, reuse, and groundwater pumping in the Nile Delta, along with a substantial decrease in Sudan irrigation demand through crop reallocation, can contribute to mitigating existing and future conflicts. Further technological improvements are needed for attaining large water demand reductions via soilless agriculture and desalination, which today cannot completely substitute reuse and groundwater contributions, whose high exploitation can induce relevant environmental risks.

1. INTRODUCTION

Deliverable D4.3 (Efficient WEF planning portfolios) is the report describing the design of efficient WEF planning portfolios under current and future scenarios. The document builds on the previous reports produced in WP4, namely D4.1 (Candidate portfolios and evaluation indicators for WEF Nexus analysis) and D4.2 (Meso level model). The work is an outcome of Task T4.3, in which the main objective is the design efficient planning portfolios based on the options identified in D4.1 under current and future scenarios as suggested by WP2. The design of the efficient portfolios relies on state-of-the-art multi-objective optimization methods coupled with advanced visual analytics tools to enable the exploration of large multidimensional spaces to explore multi-sectoral trade-offs and negotiate potential compromise alternatives.

The broader goal of WP4 is to develop a Decision-Analytic Framework (DAF) running at the river basin scale. The workflow of WP4 and its interconnections with the other WPs are illustrated in Figure 1. It relies on a detailed characterization of different innovative technological solutions demonstrated in WP5 at the micro-level (e.g., aquaponics) and a realistic representation of macro-scale processes and regional policies influencing river basin dynamics in terms of land use, water and energy supply, and ecosystem services (WP2, WP3). Besides, the case study assessments and participatory processes initiated by WP6 support our activities, integrating stakeholders (SHs) views and interests to shape our analyses.

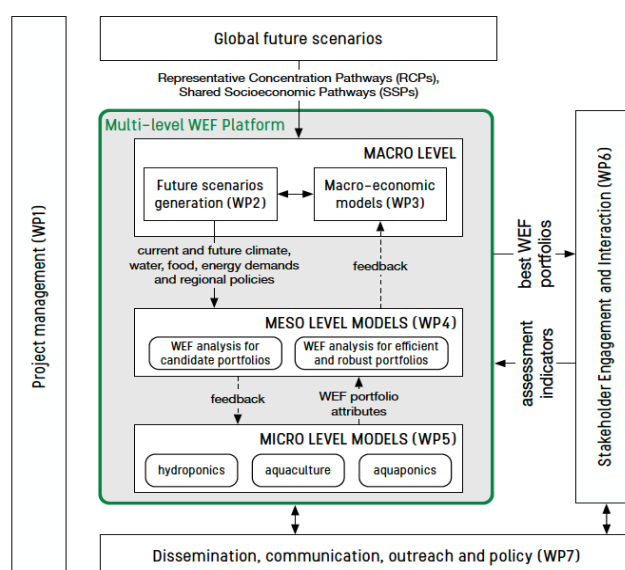


Figure 1– AWESOME project structure.

Specifically, the DAF employs a strategic river model coupled with an optimization engine (see D4.2): the river model is a parsimonious model conceptualising the main natural processes and human decisions at the whole river basin scale; the optimization engine implements a simulation-based optimization via multi-objective evolutionary algorithms (Maier 2014), which iteratively improves a set of candidate solutions in terms of their performance estimated via simulation of the strategic model at the meso level with respect to the selected evaluation indicators. In this deliverable, we

expand the preliminary assessment of some candidate portfolios reported in D4.2 by designing a large set of efficient portfolios that explore the multidimensional synergies and trade-offs across the evaluation indicators formulated in D4.2. The efficient portfolio design is performed for a historical scenario, represented by observed water availability and demand, and for a future scenario, which includes projections of hydroclimatic and socio-economic conditions.

The report is structured as follows: the next section describes the Decision Analytic Framework, Section 3 describes the components of the considered future scenario, while Section 4 reports the results of the experiments performed.

2. THE NILE RIVER BASIN

The Nile is one of the largest and most contentious river basins in the world. It is located in Northeast Africa and covers a surface of more than 3 million km² shared by eleven countries, i.e., Burundi, Democratic Republic of Congo, Egypt, Eritrea, Ethiopia, Kenya, Rwanda, South Sudan, Sudan, Tanzania, and Uganda. The Nile waters originate from the Ethiopian highlands and its major tributaries are the Blue Nile, which contributes alone 60% to its runoff, and the White Nile. The two rivers convey into the Main Nile downstream of Khartoum in Sudan, which then flows into Egypt and the Mediterranean Sea.

The climate along the NRB ranges from the Mediterranean near the northern coast to arid and semi-arid in Egypt and Sudan to subtropical and tropical with considerable precipitation in Ethiopia (Taye 2015). One unique feature of the Nile is that for almost half of its course, it flows through arid areas with no effective rainfall and substantial evaporation losses (Sutcliffe 2018). Substantial precipitation occurs in the East African lake region and southwestern Ethiopia, which receives an annual rainfall greater than 1,000 mm, while the rest of the basin receives less than 700 mm per year, with Egypt as the last place, accounting for less than 200 mm per year (Atlas 2016). The deep climate and topographic differences, the high interannual and spatial hydrologic variability, and the transboundary nature of the NRB contribute to its intrinsic complexity.

The lack of cooperation and a shared agreement that regulates the use of Nile water exacerbates international tensions. The 1959 Treaty signed by Egypt and Sudan is based on the long-term annual runoff of the Nile 84.0 BCM, which allocates water as follows: 55.5 BCM to Egypt, 18.5 BCM to Sudan and 10 BCM assumed to be lost by evaporation from Lake Nasser (Howell 1994) (Elsayed 2020). Later in 1970, the High Aswan Dam was built, which is characterised by a total storage volume of 162 BCM and an installed capacity of 2100 MW, also used to supply water in the Nile Valley and Delta for irrigation, domestic, and industrial uses. After the High Aswan Dam, no new large storage reservoirs were constructed until 2009, when Ethiopia completed the Tekeze dam with a capacity of 9.29 BCM, followed by the Merowe dam in Sudan with its 12.39 BCM of water volume, with an installed capacity of 1250 MW. The GERD construction started in 2011 on the Blue Nile in Ethiopia with the main purpose of power generation. The GERD is the largest hydroelectric power generation facility in Africa and the fifth largest in the world, accounting for a total storage of 74 BCM, an installed capacity of 5150 MW, and an annual energy generation of approximately 16 TWh (Wheeler 2020). Irrigation is the other crucial sector that plays an important role in the water management landscape of the NRB, where agriculture dominates all other water uses and is expected to increase in the future, especially in Egypt (Multsch 2017) (Nikiel 2021). The inefficient irrigation

management, however, results in a substantial increase in water demand and a fiercer competition with hydropower production (Verhagen 2021). Egypt accounts for the highest cropping intensity with an actual cropped area estimated at 6.4 million ha - approximately 79% of the total in the NRB (Atlas 2016). Most agricultural land is located in the Nile Valley and Delta, while some are also present in desert areas as part of the land reclamation project started in 1952 (Adriansen 2009). The high productivity of the soil and the suitable climate allowed the cultivation of a wide variety of crops such as grains, pulses, fibers, oil, seeds, sugar, vegetables, fodder, and tree crops. The 97% of water available for irrigation comes from the river with eight barrages diverting the water released from the High Aswan Dam to eleven irrigation districts. The remaining 3% of irrigation water is from precipitations, groundwater extraction, and drainage reuse (statistics 2017). Even though such secondary sources account for a small percentage of the total water balance of Egypt, they hold great potential in a country that faces growing water scarcity issues. Table 1 shows the water balance of Egypt's water resources and water uses considered in this study.

Table 1 Egyptian Water Balance 2017 (Arab Republic of Egypt 2017)

| Sectorial indicator | BCM/y |
|---|-------|
| Available renewable fresh-water resources | 59.60 |
| Domestic water consumption | 2.70 |
| Industrial water consumption | 1.41 |
| Agricultural water consumption | 40.69 |

3. MESO LEVEL DECISION-ANALYTIC FRAMEWORK

The results of this Deliverable are obtained through a Decision-Analytic Framework (DAF) running at the river basin scale (s. Figure 2). It relies on a detailed characterisation of different innovative technological solutions demonstrated in WP5 at the micro-level (e.g., aquaponics) and a realistic representation of macro-scale processes and regional policies influencing river basin dynamics in terms of land use, water and energy supply, and ecosystem services according to both current and future scenarios (WP2, WP3). Besides, the case study assessments and participatory processes initiated by WP6 support our activities, integrating stakeholders (SHs) views and interests to shape our analyses. The combination of systems analysis methods and advanced a posteriori multi-objective evolutionary optimization algorithm (MOEAs) allows the discovery of a set of efficient solutions and associated performance with respect to the WEF multi-dimensional assessment space, where SHs and policy makers are able to explore multi-sectoral trade-offs and negotiate potential compromise alternatives. The DAF employs a strategic river model coupled with an optimization engine: the river model is a parsimonious model conceptualizing the main natural processes and human decisions at

the whole river basin scale. The optimization engine implements a simulation-based optimization via multi-objective evolutionary algorithms (Maier 2014) which iteratively improves a set of candidate solutions in terms of their performance, estimated via simulation of the strategic model, with respect to a subset of selected evaluation indicators (i.e. design indicators).

In the following sub-sections, we provide an overview of the DAF, while a detailed description of its components is reported in Deliverable D4.2 (Meso Level Model), where the strategic model is used to map the candidate portfolios identified in Deliverable D4.1 (Candidate portfolios and evaluation indicators for WEF Nexus analysis) into their associated performance as quantified by the evaluation indicators. In this Deliverable, we use the DAF to design efficient portfolios that better handle synergies and trade-offs across the WEF Nexus.

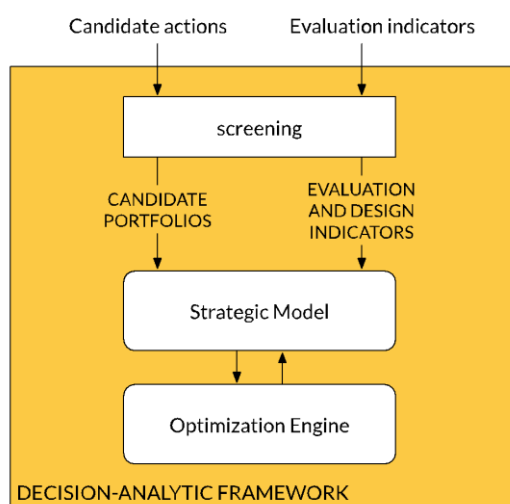


Figure 2 – Strategic DAF model at the meso level.

STRATEGIC MODEL FOR THE NILE RIVER BASIN

The strategic model developed for the NRB integrates two main components:

- **Water Supply model** that supports the analysis of the operating policies of the main dams along the Nile River, along with the water abstraction for the irrigation areas in Sudan and the water supply downstream of the High Aswan Dam.
- **Water Demand model** that investigates alternative combinations of water demand interventions, namely reuse, groundwater, aquaponics/hydroponics and desalination, to reduce the water demand downstream of the High Aswan Dam.

The Water Supply model focuses on describing the branch of the Blue Nile from the Grand Ethiopian Renaissance Dam (GERD) to Khartoum and the Main Nile until it reaches the Mediterranean Sea. In the system (s. Figure 3), three dams (GERD, MER and HAD) and four irrigation areas are modelled following the approach illustrate in the previous subsections.

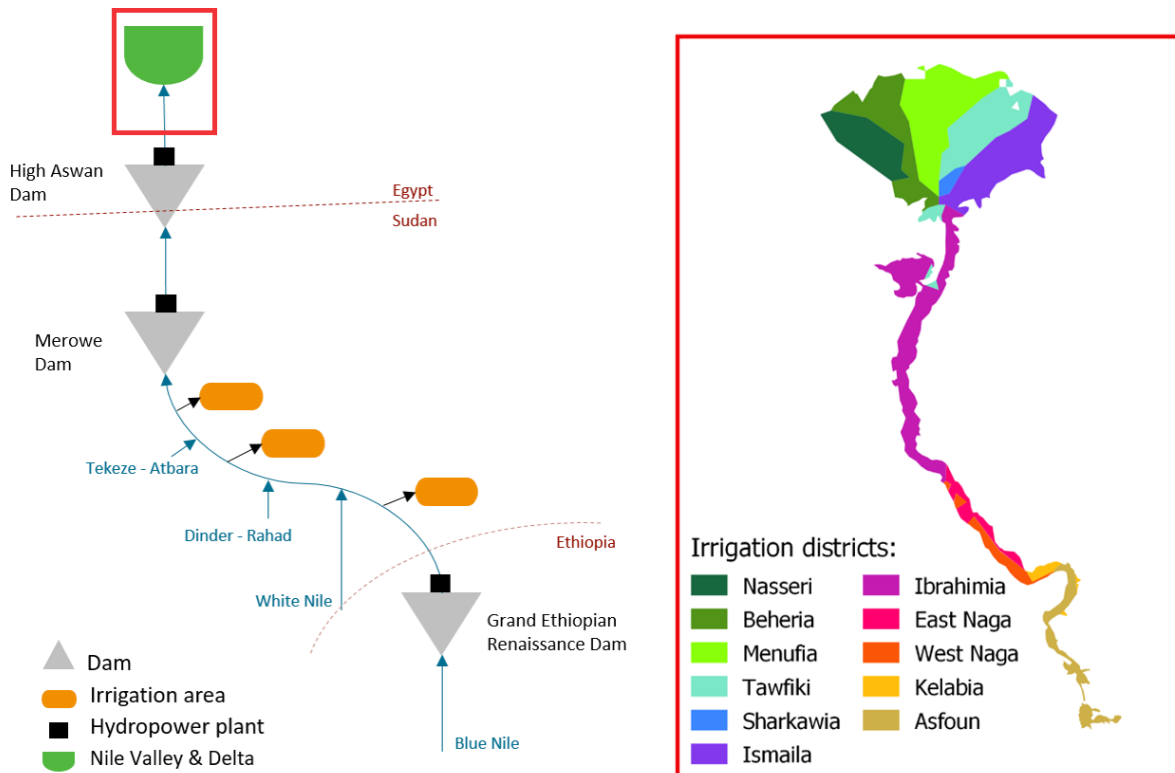


Figure 3 – Schematic representation of the Nile River Basin model structure.

The Water Demand model focuses on the last stretch of the river, flowing from the HAD to the Mediterranean Sea. The area is modelled considering eleven irrigation districts (s. Figure 3), whose water demand can be satisfied by the water released by the HAD or through the implementation of different water demand measures, namely water reuse, groundwater, hydroponics/aquaponics and desalination.

The conflicting interests among different stakeholders were modelled by formulating a set of evaluation indicators associated to the different components of the WEF Nexus as detailed in Table 2 of D4.2. A subset of these evaluation indicators is used in the DAF as objective functions for the design of efficient portfolios.

The Water Supply optimization is a multi-objective planning and management problem that maximizes the total hydropower production at the basin scale ($J^{E,TOT}$) and minimizes the total irrigation deficit in the three districts in Sudan ($J^{Irr,Sudan}$) as well as the total irrigation deficit of Egypt ($J^{Irr,Egypt}$). The complete formulation of these objectives is reported in the deliverable D4.2. In addition, the problem also minimizes the volumes of water demand reduction to implement downstream of HAD ($J^{RED} = \gamma$). The Water Supply problem can be then formulated as follows:

$$\max_{p,\gamma} J = | J^{E,TOT}, -J^{Irr,Sudan}, -J^{Irr,Egypt}, -J^{RED} |$$

where the decision variables are the policies (p) for the operations of the three dams and water diversions to the irrigation areas in Sudan, and the planned irrigation demand reduction (γ). This problem is dynamically constrained by the three reservoirs dynamics (s. D4.2 for details).

A variant of the Water Supply optimisation is explored by assuming a non-cooperative scenario between Ethiopia and the downstream countries. This optimisation is carried out in two steps, first by optimising the GERD's operations and targeting the maximization of hydropower production of the GERD. Since this dam is upstream of the system, it can make individualistic decisions without being affected by the downstream system. From this first optimization, we obtain the policy that maximises the GERD's hydropower production and the associated trajectory of releases that cross the border and flow into Sudan, thus conditioning the water management of the downstream water infrastructures. Then, we run a second optimization focused on the operations of MER and HAD along with the Sudanese irrigation diversions, and targeting the maximisation of the aggregate hydropower production of HAD and MER, the minimisation of the deficits of Egypt and Sudan, and the minimization of water demand reduction downstream of HAD.

The Water Demand optimization problem is formulated as a multi-objective planning problem that minimises the annual reuse of drainage water (J^R), the annual groundwater use distance from the sea to avoid saline water intrusion (J^{GW2}), construction and operation cost of soilless agricultural systems (J^{Aq1}), construction and operation cost of desalination plants (J^{D1}), desalination water supply cost (J^{D2}), desalination water distribution cost (J^{D3}). Again, the complete formulation of these objectives is reported in the deliverable D4.2. Moreover, the Water Demand problem includes an additional objective that penalizes the connections between districts for the distribution of desalinated water (J^P), it is formulated as a penalty for transporting desalinated water to a district where there is already a desalination plant and for not using desalinated water in a district where a desalination plant is built:

$$J^P = \sum_{i=1}^{11} \sum_{d=1}^{11} g_{id}^P$$

$$g_{id}^P = \begin{cases} g_{id}^P = 1, & \text{if } \sum_{d=1}^{11} u_{id}^D \neq 0 \text{ and } u_{da}^D = 0 \\ g_{id}^P = 1, & \text{if } u_{id}^D \neq 0 \text{ and } i \neq d \text{ and } u_{ii}^D \neq 0 \end{cases}$$

The Water Demand problem can be then formulated as follows:

$$\min_u J = |J^R, J^{GW2}, J^{Aq1}, J^{D1}, J^{D2}, J^{D3}, J^P|$$

where the decision variables are the volumes of water demand reductions allocation to reuse, groundwater, hydroponics/aquaponics and desalination. Specifically, each district is associated with one decision variable to define the water reuse, one for the groundwater extracted and one for the implementation of hydroponics/aquaponics. Besides, an 11x11 matrix represents the decisions associated with the desalination technology: the element in row d and column i of the matrix defines

the volume of desalinated water produced in the d -th district that is delivered to the i -th district. In total, the Water Demand problem includes 154 decision variables.

OPTIMIZATION ENGINE

The Water Supply problem is solved using the Evolutionary Multi-Objective Direct Policy Search (EMODPS) method (M. e. Giuliani 2015), while the Water Demand implements the Borg Multi-Objective Evolutionary Algorithm (Hadka 2013).

EMODPS (s. Figure 4) is a Reinforcement Learning approach that combines direct policy search, non-linear approximating networks and multi-objective evolutionary algorithms. The reservoir operating policies are defined as Gaussian radial basis functions (Buşoniu 2011), while the irrigation diversions are operated according to non-linear hedging rules. The advantage of using EMODPS against other optimal control methods (M. L. Giuliani 2021) is the possibility of designing the coordinated control across multiple reservoirs alleviating the well-known curse of dimensionality (M. L. Giuliani 2021). Moreover, EMODPS enables the computation of an approximation of the Pareto front in a single run of the algorithm, which supports the exploration of multidimensional trade-offs between conflicting objectives (M. H. Giuliani 2014). To perform the optimization, we use the self-adaptive Borg Multi-Objective Evolutionary Algorithm, which has been shown to be highly robust in solving multi-objective optimal control problems, where it met or exceeded the performance of other state-of-the-art MOEAs (Zatarain Salazar 2016). Borg MOEA differs from traditional evolutionary algorithms because the application of these operators is not bound to a fixed probability of occurrence. Their employment is adaptively adjusted during the optimization considering their ability to generate efficient solutions (Hadka 2013).

The Water Supply optimization was run for 2 million function evaluations. To improve solution diversity and avoid dependence on randomness, the final set of optimal policies is obtained as the set of nondominated solutions identified from 10 random optimization trials. The total number of decision variables considered amounts to 101, 94 of which are included in the RBFs, 6 parameters are set for Sudan irrigation and 1 for irrigation reduction control. From the final Pareto front, few solutions are selected, and their corresponding values of water demand reduction are used in the second optimization.

The Water Demand optimization was run for 1 million function evaluations.

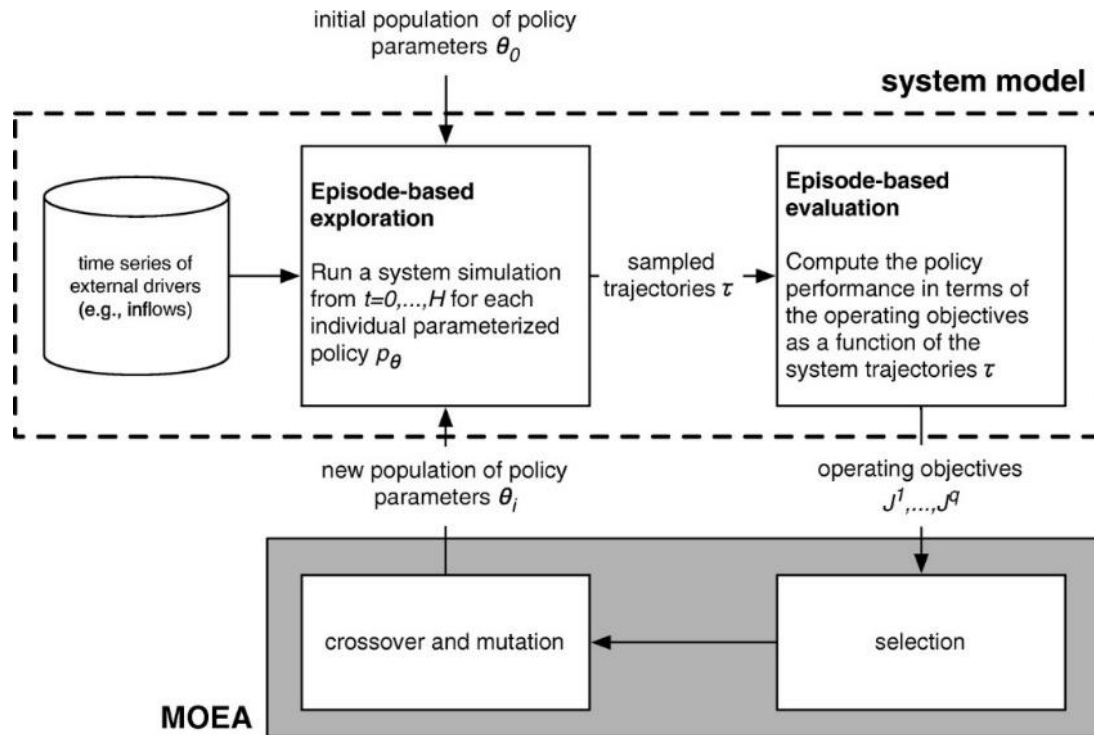


Figure 4 – Schematization of the Evolutionary Multi-Objective Direct Policy Search (EMODPS) approach; dashed lines represent the model of the system and the grey box represents the multi-objective evolutionary optimization algorithms (MOEA) (M. e. Giuliani 2015).

4. FUTURE SCENARIOS

Water Supply and Water Demand models are optimized both for a historical scenario, represented by observed water availability and demand, and for a future scenario, which includes projections of hydroclimatic and socio-economic conditions. These projections were generated as part of the work of WP2:

- climate projections for three selected Representative Concentration Pathways (RCPs) (Pachauri s.d.) are described in the Deliverable D2.2;
- future population projections according to the Shared Socioeconomic Pathways (SSPs) (Masson-Delmotte 2021) are presented in Deliverable D2.1;
- current and future crops' water needs and production are illustrated in Deliverable D2.3.

In this deliverable, we consider RCP4.5 and SSP2 as the reference future scenario: RCP4.5 corresponds to a business-as-usual scenario, where the radiative forcing rises until 2050 to stabilise in the second half of the century; SSP2 is defined as the medium development scenario, whereby population, economic and technological trends do not deviate strongly from historical ones. The other scenarios and their associated uncertainties will be analysed in Deliverable D4.4.

4.1 URBAN DEMAND

Demographic projections were produced under all SSP scenarios (s. D2.1). These projections were generated under the Bayesian population model developed by (Ševčíková 2016) which produces probabilistic projections for the population pyramids of both genders. This model is a stochastic extension in a Bayesian fashion of the typical logistic-type model used by UN for predicting population and it relies on three main modelling components: (a) fertility rate, (b) life expectancy and (c) migration. At the upper layer, the population model aggregates the aforementioned components, which are modelled separately under appropriate Bayesian modelling considerations (for more details please see D2.1, (Ševčíková 2016) and references therein), to provide the population trajectories. These components were appropriately modified to distinguish between the different SSP scenarios, and therefore probabilistic projections for population (and the relevant components, e.g. fertility rate, life expectancy, etc) were derived for all countries in the area of interest (Mediterranean region) under the five different socio-economic scenarios till the year 2100. These data samples are used to estimate the median population trajectories per scenario.

For the purposes of D4.3, the SSP2 median trajectory and the relevant increase rate of population (using as reference year 2020) is used for modelling and predicting water demand for Egypt as reported in Table 22.

Table 2 – Illustration of population projection data for Egypt under the SSP2 scenario used for water demand estimation.

| Year | Population | Increase Rate |
|------|------------|---------------|
| 2020 | 102334.403 | 1.000 |
| 2025 | 111687.149 | 1.091 |
| 2030 | 120708.958 | 1.180 |
| 2035 | 130124.367 | 1.272 |
| 2040 | 139977.088 | 1.368 |
| 2045 | 149874.35 | 1.465 |
| 2050 | 159364.717 | 1.557 |
| 2055 | 168306.793 | 1.645 |
| 2060 | 176712.153 | 1.727 |
| 2065 | 184669.609 | 1.805 |
| 2070 | 192150.807 | 1.878 |
| 2075 | 199064.02 | 1.945 |
| 2080 | 205442.541 | 2.008 |
| 2085 | 211163.126 | 2.063 |
| 2090 | 216028.955 | 2.111 |
| 2095 | 220097.473 | 2.151 |
| 2100 | 223283.056 | 2.182 |

4.2 IRRIGATION DEMAND SCENARIOS

Crop water demands were estimated under the climate scenario RCP4.5 and population projection of SSP2 by first considering the current crop distribution and, secondly, different options of crop reallocation. Specifically, we used the spatially distributed agro-hydrological model WATNEEDS (Chiarelli 2020) to assess the daily water balance and the volumes of water needed to cover crop's evapotranspiration during the growing period without experiencing water stress. Green water requirement is met by precipitation, while blue water requirement is met by irrigation, when precipitation alone cannot completely satisfy the crop requirement. The WATNEEDS model works at a spatial resolution of 5 arcmins at the equator and can simulate both historical and future crop demands. We implemented cropland reallocation scenarios for Egypt and Sudan, both at the country scale and at the basin scale (meso scale). Cropland reallocation is performed with the aim of enhancing agricultural production and preserving the consumption of irrigation water. Results showed that in Egypt, due to the high percentage of irrigated land (98% of the current cropland is irrigated), it has been possible to increase production without exceeding the current blue water consumption, or consuming an additional amount of max 5% only. In Sudan, due to the reduced availability of agricultural land, an increase in production has resulted impossible without assuming an agricultural expansion. We explored a hypothetical scenario of irrigation expansion for Sudan, considering potential irrigation areas, provided by Eastern Nile Technical Regional Office (ENTRO (Repository s.d.)). However, the resulting consumption of irrigation water exceeded the current consumption (up to 50%), proportionally to the newly harvested hectares, resulting in a non-sustainable scenario in terms of water consumption. On the other hand, model results show that the crop reallocation performed at the entire Nile River Basin scale entails higher productivity and lower blue water consumption with respect to the country scale, and, thus, offers a more sustainable scenario of resource optimization.

Figure 5 shows the spatially distributed blue water consumption in the Nile River Basin, for the baseline and for the implemented scenarios, with (I1) and without (I1) agricultural intensification. The simulated crop replacement scenarios over the entire Nile River Basin show the potential to save up to 21% of the cropland and 42% of irrigation water, when agricultural intensification is applied (scenario I1, Figure 5), maintaining the current agricultural production. Hence, this scenario appears a good candidate for representing plausible future irrigation demands.

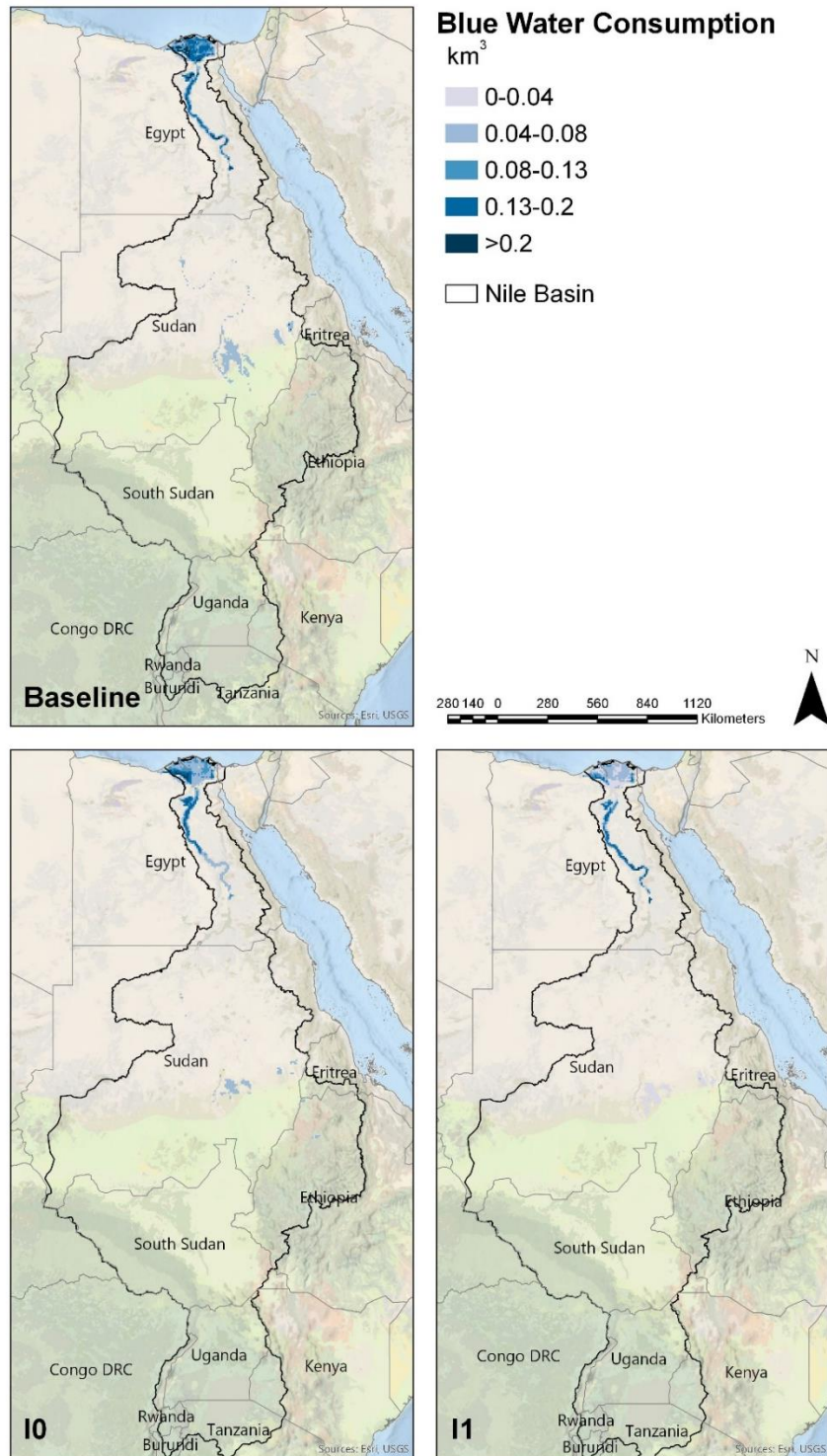


Figure 5 – Spatially distributed (5 arc-minutes resolution) blue water consumption in km³ in the Nile River Basin, for the baseline scenario (top left) and for the reallocation scenarios with current yields (I0, bottom left) and with agricultural intensification (I1, bottom right).

4.3 STREAMFLOW PROJECTIONS

To simulate the strategic model under future climatic conditions, it is necessary to generate the streamflow corresponding to the projected precipitation and temperature conditions for all the modelled tributaries of the Nile River, i.e., Blue Nile, White Nile, Dinder, Rahad, Tekeze and Atbara. Giving the large extension and climatic heterogeneity of the NRB, the studied area is divided into four sub catchments shown in Figure 6, each acting as separated hydrological units: Blue Nile, White Nile, Tekeze-Atbara and Dinder-Rahad subbasins.

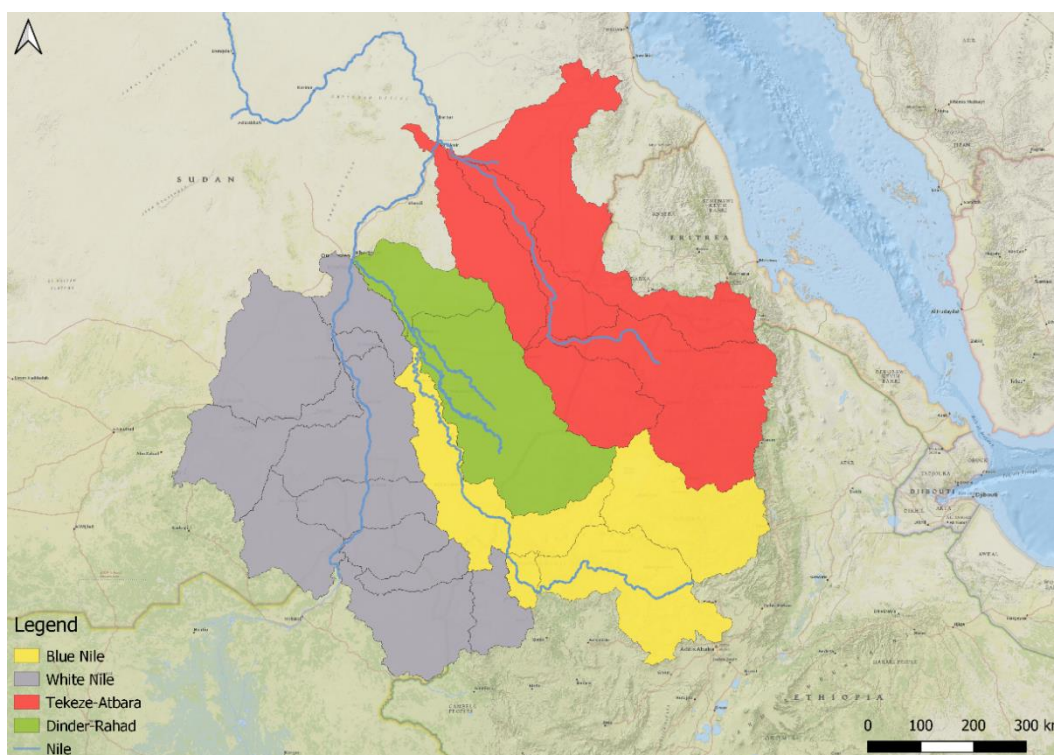


Figure 6 – Sub-basins of the Nile River Basin acting as primary hydrological units.

3.3.1 Hydrologic modelling

The Hydrologiska Byrans Vattenbalansavdelning (HBV) model (S. & Bergström 1976) (S. Bergström 1995) is a lumped rainfall-runoff model requiring two inputs, temperature and precipitation, to generate river discharge. The model relies on 5 state variables and 12 parameters that need to be calibrated for each subbasin. The model was calibrated using CHIRSP and CHIRTS dataset (Barbara s.d.) reporting, respectively, daily precipitation and temperature at high resolution (0.05° resolution over Africa) ranging from 1982 for precipitation and 1983 for temperature until 2005. The streamflow data used for the model calibration and validation are monthly historical observations that range from 1965 until 2011. The available data time series, composed of 22 years from 1983 until 2005, is divided into two subsets of 15 (1983-1998) and 7 (1999-2005) years, used respectively for calibration and validation. The fitness of the model in calibration and validation is estimated with two metrics, i.e., the Pearson correlation (r) and the Nash Sutcliffe Efficiency (NSE). Correlation can range from -1 to 1, where a correlation equal to -1 indicates a negative linear correlation and 1 is a positive linear correlation. The Nash–Sutcliffe efficiency is calculated as one minus the ratio of the error variance

of the modelled time-series divided by the variance of the observed time-series. This metric ranges from $-\infty$ to 1, where 1 indicates a perfect match between modelled and observed.

The values of the two metrics obtained in calibration and validation are shown in the Table 33.

Table 3 – Values of the NSE and Pearson coefficient metrics for the calibration and validation with the HVB model for the Blue Nile, White Nile, Tekeze-Atbara and Dinder-Rahad sub-basins.

| Sub-basin | Calibration | | Validation | |
|---------------|-------------|------|------------|------|
| | R | NSE | R | NSE |
| Blue Nile | 0.95 | 0.75 | 0.85 | 0.60 |
| White Nile | 0.002 | -3.6 | -0.13 | -5.4 |
| Tekeze-Atbara | 0.84 | 0.71 | 0.80 | 0.51 |
| Dinder-Rahad | 0.86 | 0.74 | 0.75 | 0.57 |

For the Blue Nile sub-basins, Tekeze-Atbara and Dinder-Rahad, the HVB model provides good results, although it is possible to note an appreciable deterioration of the metrics in the transition from calibration to validation and some discrepancies in simulated and observed peaks in Figure 7. Conversely, the results for the White Nile basin are much worse and the model seems unable to reproduce the inflow of this river whose historical trend shows several anomalies that are attributable to the presence of the Jebel Aulia Dam, that is not included in our models. To reduce the error in the peaks simulation and improve the generation of White Nile inflow, additional modelling effort is required. We designed a single-layer, feedforward neural network (ANN) aimed at modeling the HBV residuals.

The design of an ANN requires to specify the inputs of the network as well as the number of neurons in the hidden layer. Three metrics were selected for the network calibration and validation: R, coefficient of determination (R^2) and root mean square error (RMSE). R^2 is a measure of the strength of the relationship between observed values and simulated, this metric ranges from 0 to 1, where 1 indicates perfect correspondence between observation and simulation, while RMSE is the standard deviation of the residuals, it gives a measure of how spread out the residuals are, it values ranges from 0 to ∞ , where 0 corresponds to a model without residuals. R and R^2 are maximised while RMSE is minimized. The dataset is again subdivided into two subsets of 15 and 7 years for the calibration and validation of the ANN. Since the length of the available datasets is quite limited, we decided to use a k-fold cross-validation. We divided the original series available for calibration into 3 subsets, each of 5 years, which are used for calibration except for one which is used in validation. The procedure is repeated until the model has been validated on all the 3 sets. Once all experiments have been performed, the best ANN architecture can be chosen; after a final training over the entire 15 years, the resulting model was combined with the HBV and validated on the last 7 years.

In our study, we tested four networks, which differ according to the inputs fed into them (s. the second column of Table 4). Table 4 report the values of the metrics for the combined HBV+ANNs models validation on the held-out seven years. The results show that the ANNs can improve the HBV model simulation, with the ANN with three inputs (observed inflows, date and precipitation, s. rows with yellow background) returning the highest values for all three metrics in all the subbasins.

Table 4 – Values of the Pearson coefficient (R), R^2 and RMSE metrics obtained for the validation of different architecture of ANN for the bias correction for the streamflows of Blue Nile, White Nile, Tekeze-Atbara and Dinder-Rahad.

| Sub-basin | Model | Inputs of ANN | N° of neurons | R | R^2 | RSME |
|----------------------|------------|---|---------------|--------|-------|------|
| Blue Nile | HBV | | | 0.85 | 0.44 | 486 |
| | HBV + ANN1 | HBV simulation | 7 | 0.87 | 0.51 | 456 |
| | HBV + ANN2 | HBV simulation and date | 4 | 0.95 | 0.83 | 272 |
| | HBV + ANN3 | HBV simulation, date and precipitation | 5 | 0.97 | 0.85 | 251 |
| | HBV + ANN4 | HBV simulation, date, precipitation and temperature | 6 | 0.96 | 0.79 | 297 |
| White Nile | HBV | | | -0.13 | -0.04 | 513 |
| | HBV + ANN1 | HBV simulation | 5 | -0.025 | -0.29 | 268 |
| | HBV + ANN2 | HBV simulation and date | 3 | 0.70 | 0.13 | 259 |
| | HBV + ANN3 | HBV simulation, date and precipitation | 4 | 0.74 | 0.19 | 213 |
| | HBV + ANN4 | HBV simulation, date, precipitation and temperature | 5 | 0.71 | 0.17 | 260 |
| Tekeze-Atbara | HBV | | | 0.80 | 0.45 | 486 |
| | HBV + ANN1 | HBV simulation | 7 | 0.77 | 0.51 | 456 |
| | HBV + ANN2 | HBV simulation and date | 4 | 0.93 | 0.83 | 272 |
| | HBV + ANN3 | HBV simulation, date and precipitation | 5 | 0.93 | 0.85 | 251 |
| | HBV + ANN4 | HBV simulation, date, precipitation and temperature | 6 | 0.93 | 0.79 | 297 |
| Dinder-Rahad | HBV | | | 0.75 | 0.57 | 124 |
| | HBV + ANN1 | HBV simulation | 7 | 0.83 | 0.68 | 115 |
| | HBV + ANN2 | HBV simulation and date | 3 | 0.93 | 0.75 | 98 |

| | | | | | | |
|--|------------|---|---|------|------|-----|
| | HBV + ANN3 | HBV simulation, date and precipitation | 5 | 0.94 | 0.77 | 91 |
| | HBV + ANN4 | HBV simulation, date, precipitation and temperature | 6 | 0.94 | 0.71 | 104 |

The comparison between the observed streamflow, HBV simulation and HBV simulation corrected with best ANN is shown in Figure 7. Again, one can see the contribution made by ANN in improving the simulation of inflows, especially in the reproduction of peaks.

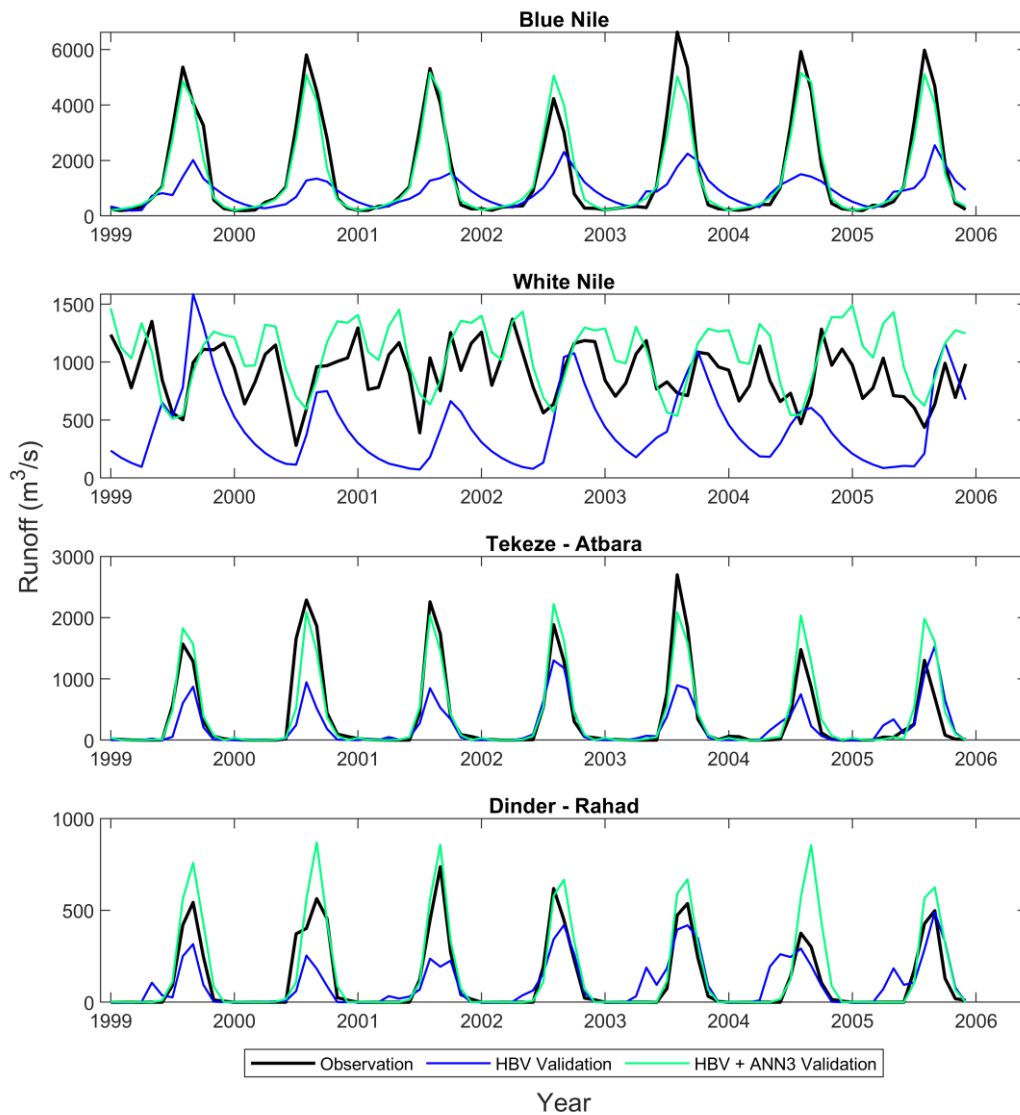


Figure 7 – Observed and simulated streamflow over the validation period for Blue Nile, White Nile, Tekeze – Atbara, Dinder – Rahad. In the figure are compared the observed streamflow (black) with the one simulated by the HBV model (blue) and HBV model corrected with ANN (green).

3.3.2 Climate scenarios

To generate the future inflows of the main tributaries of the Nile using the HVB+ANN model, we consider the time series of temperature and precipitation from 2007 to 2100 for the scenario RCP4.5. Under this scenario, precipitation in all sub-basins shows a decreasing trend over time during the annual peak, in the summer months, and a slight increase in the autumn months. Moreover, this scenario is affected by high interannual variability, especially in summer. The Blue Nile seems to be the most affected by the decrease in precipitation, with projected summer precipitation peaks of 8 mm/d below the historical value of 9.5 mm/d. The temperature is instead expected to rise gradually over time, with an average increase of between 2-3 °C at the end of the century compared to the current situation. More details are available in D2.2.

These projected trajectories are then used as input for the HBV+ANN model described in the previous subsection. The model will thus simulate the streamflow of the four tributaries from 2007 to 2100 to be used as input to the Water Supply model. The simulated outputs are shown in Figure 8 a monthly streamflow averaged over 10-year intervals and compare with the historical average, marked in black in the figure. We note a non-linear decrease in the curve over time, with some inter-annual variations. Furthermore, there is a strong decrease in inflow in the summer season for Blue Nile, Tekeze-Atbara and Dinder-Rahad, in agreement with what was obtained for the rainfall projections. In the Blue Nile and Tekeze-Atbara is registered a slight streamflow increase in the autumn months, again explained by future trends of precipitations. The White Nile shows a different trend with increasing streamflow during summer and decreasing during the rest of the year.

The basin most affected by climate change is the Blue Nile, for which the model predicts a greater decrease in inflow, especially during the annual peak, than for the other sub-basins.

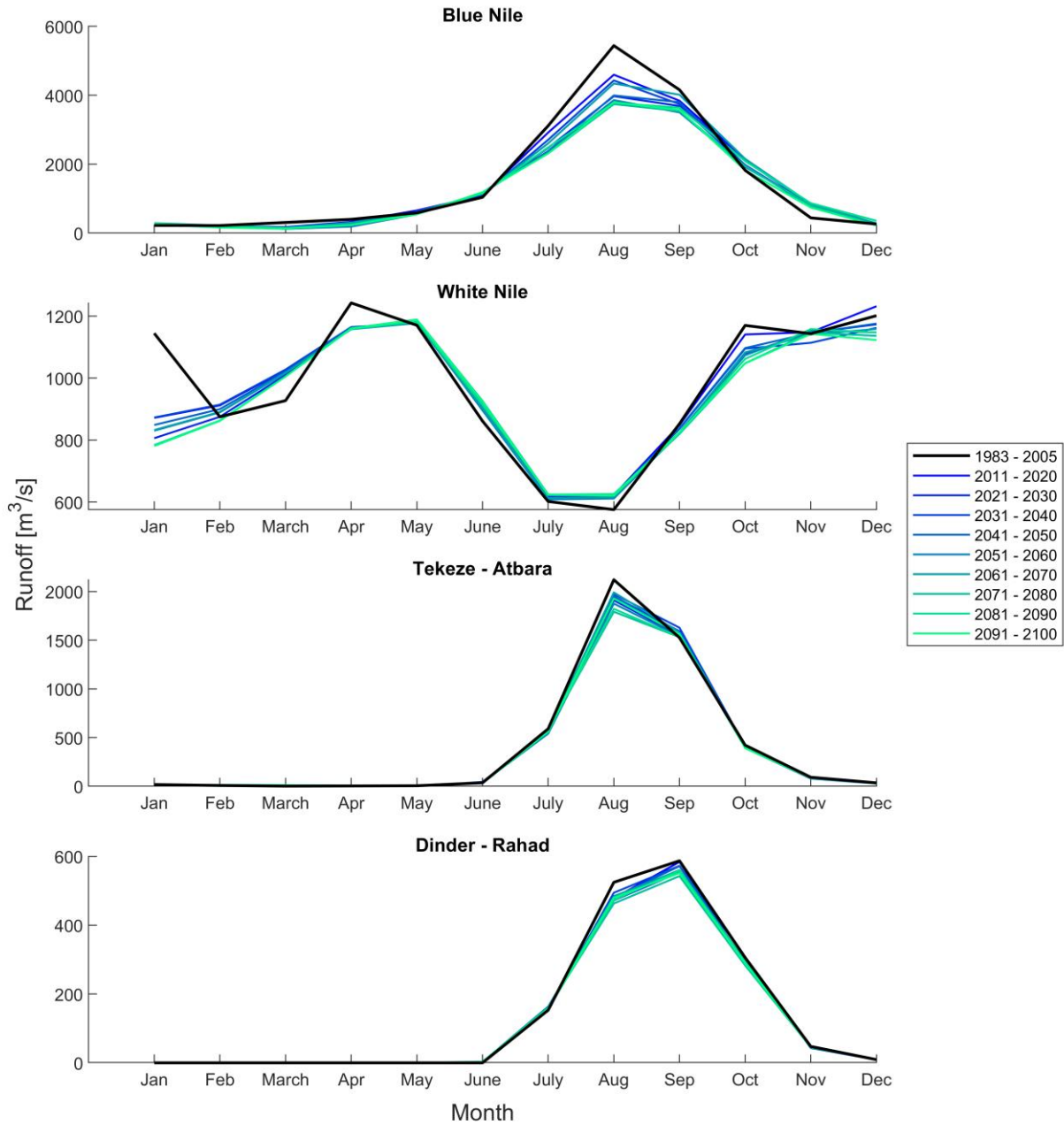


Figure 8 – Future projected streamflow for Blue Nile, White Nile, Tekeze – Atbara, Dinder – Rahad. The projections are shown as monthly averages over 10 year intervals (blue and green lines) and plotted against the historical monthly average (black line), computed for the time interval 1983-2005.

5. RESULTS

In this chapter we present and discuss the portfolios designed for the NRB. We first analyse the trade-offs obtained by the reoperation of the three main dams (GERD, MER and HAD) and the diversion policies of the irrigation districts under the current hydroclimatic conditions under a cooperative scenario between Ethiopia, Sudan and Egypt; next, we explore a second scenario assuming a non-cooperative attitude of Ethiopia with respect to the downstream countries.

Two efficient solutions of the Water Supply problem are selected from the cooperative optimization and analysed more in details by solving also the corresponding Water Demand problem to determine the allocation of the water demand measures able to balance the demand reduction obtained by the Water Supply problem. From this second trade-off analysis, we finally extract four solutions to further explore the economic and physical implications of desalination and aquaponics implementation.

Lastly, we repeat the overall procedure optimizing the Water Supply and Water Demand models under future conditions of streamflow and water demand and different cooperation scenarios between the three countries.

5.1 HISTORICAL CONDITIONS

Figure 9 shows the result of the optimisation of the Water Supply model and the synergies and trade-offs across different evaluation indicators: hydropower production at the basin scale ($J^{E,Nile}$), hydropower production in Ethiopia ($J^{E,GERD}$), hydropower production in Sudan ($J^{E,MER}$), hydropower production in Egypt ($J^{E,HAD}$), irrigation deficits of Sudan ($J^{Irr,Sudan}$) and Egypt ($J^{Irr,Egypt}$) and water demand reduction below HAD (J^{RED}). The parallel-axes plot represents a 7-dimensional space, where each axis indicates a different indicator with the direction of preferences that is upward. The ideal solution would be thus represented by a horizontal line on the top of all the axes, whereas crossing lines identifies trade-offs among indicators visualized on consecutive axes. We observe a clear trade-off between hydropower production and the Sudanese irrigation deficit, for which greater hydropower generally leads to higher deficits. The reason behind it is that the water allocated for irrigation in Sudan can reduce the water used for hydropower generation in MER and HAD. In contrast, the trade-off between hydropower production and Egypt deficit is not as evident, even if we can notice that the latter has a direct impact on the HAD power generation. Moreover, the introduction of water demand reduction downstream of HAD can lead to potential mitigation of the conflicts between irrigation and power generation.

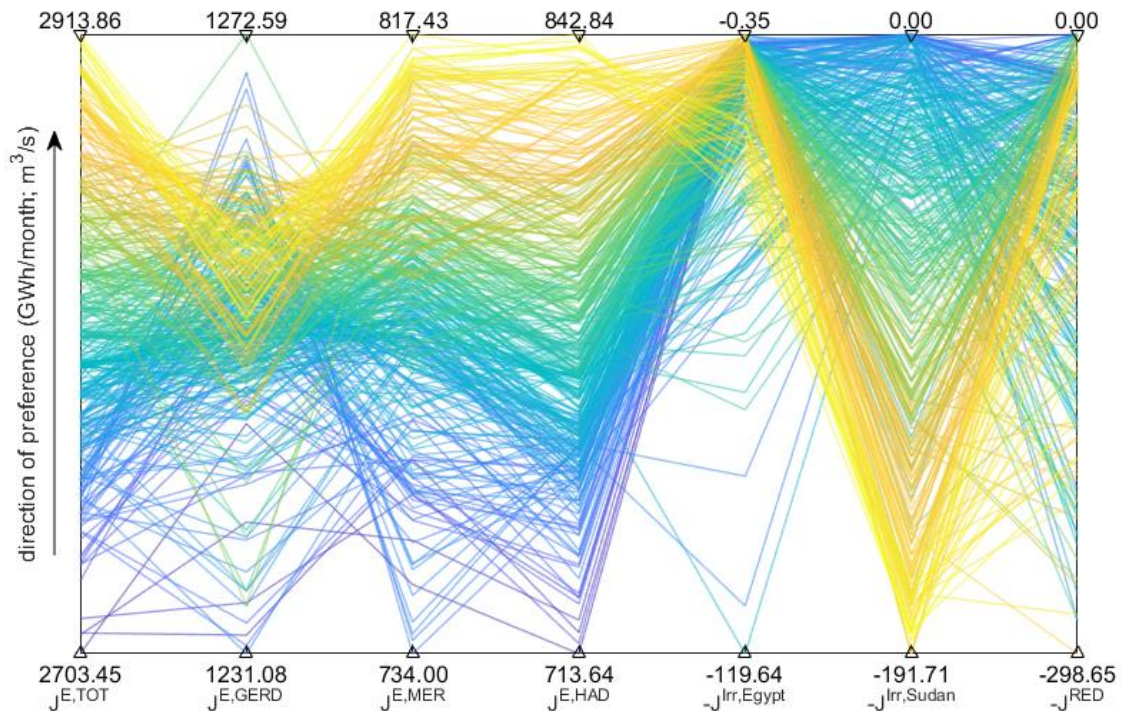


Figure 9 – Parallel plots of the Water Supply optimization showing hydropower production at the basin scale ($J^{E,TOT}$), in Ethiopia ($J^{E,GERD}$), Sudan ($J^{E,MER}$) and Egypt ($J^{E,HAD}$), Egypt irrigation deficit ($-J^{Irr,Egypt}$), Sudan irrigation deficit ($-J^{Irr,Sudan}$) and water reductions below HAD ($-J^{RED}$). The colour are assigned according to the level of energy produced at the basin scale ($J^{E,TOT}$), where yellow line corresponds to high energy productions and blue lines to low one.

Further evidence of the benefit of introducing water demand downstream of the system can be seen in Figure 10. This scatter plot shows the energy production against the overall deficit (generated by summing the Sudanese deficit with the Egyptian one), while the colour of each solution represents the value of demand reduction. The water reduction is categorized in three groups: low reduction (below $25 \text{ m}^3/\text{s}$), medium reduction (between 25 and $100 \text{ m}^3/\text{s}$) and high reduction (higher than $100 \text{ m}^3/\text{s}$). According to this representation, the best solution is positioned in the top right corner for zero deficit and maximum hydroelectric production. It is interesting to note that all the not dominated solutions in this bi-dimensional space are obtainable for high levels of water demand reduction (red circles), while moving to sub-optimal solutions the volume of water reduction decreases gradually.

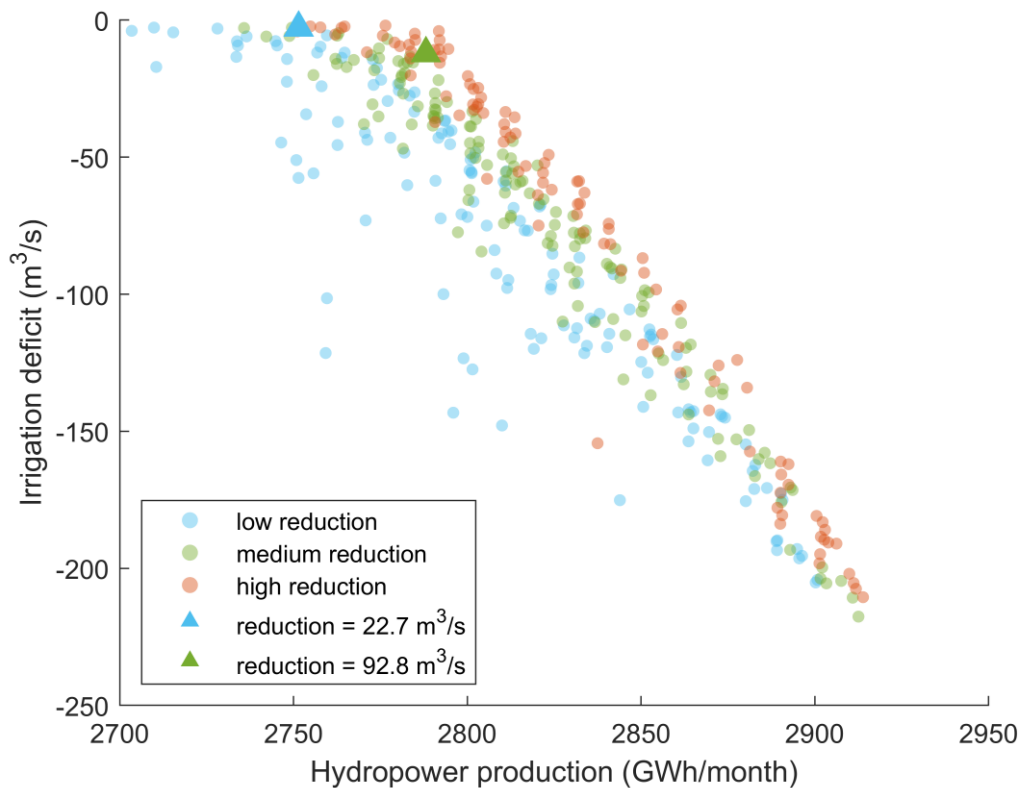


Figure 10 – Scatter plot representation of the total hydropower produced at the basin scale against the aggregated irrigation deficit of Sudan and Egypt. To each solution is associated a colour representing the volume of water reduction: blue for reduction lower than $25 \text{ m}^3/\text{s}$, green for reduction between 25 to $100 \text{ m}^3/\text{s}$ and red for reductions higher than $100 \text{ m}^3/\text{s}$. Two solution are represented as triangles one for low reduction ($22.7 \text{ m}^3/\text{s}$) and one for medium reduction ($92.5 \text{ m}^3/\text{s}$).

From these results, we selected two alternatives (triangles in Figure 10) corresponding to a low and a medium water reduction, respectively. The high-reduction alternatives have been neglected for the time being as they would require too much effort in terms of water demand measures. Both the considered solutions were chosen from the portfolios attaining low irrigation deficits, so that the implementation of water demand measures is allowing the increase of the total hydropower production by 40 GWh/m with minimum impacts on water supply.

The simulated dynamics of the three reservoirs under the selected solutions is reported in Figure 11. We observe that the portfolio implementing a medium water demand reduction (blue line) tends to keep higher water level of HAD, with this operating strategy producing a higher hydropower generation. The larger differences in the dynamics of HAD with respect to GERD and MER can be explained because HAD is located downstream of the Sudanese diversions, and it is thus more sensitive to the irrigation supply than the two upstream dams.

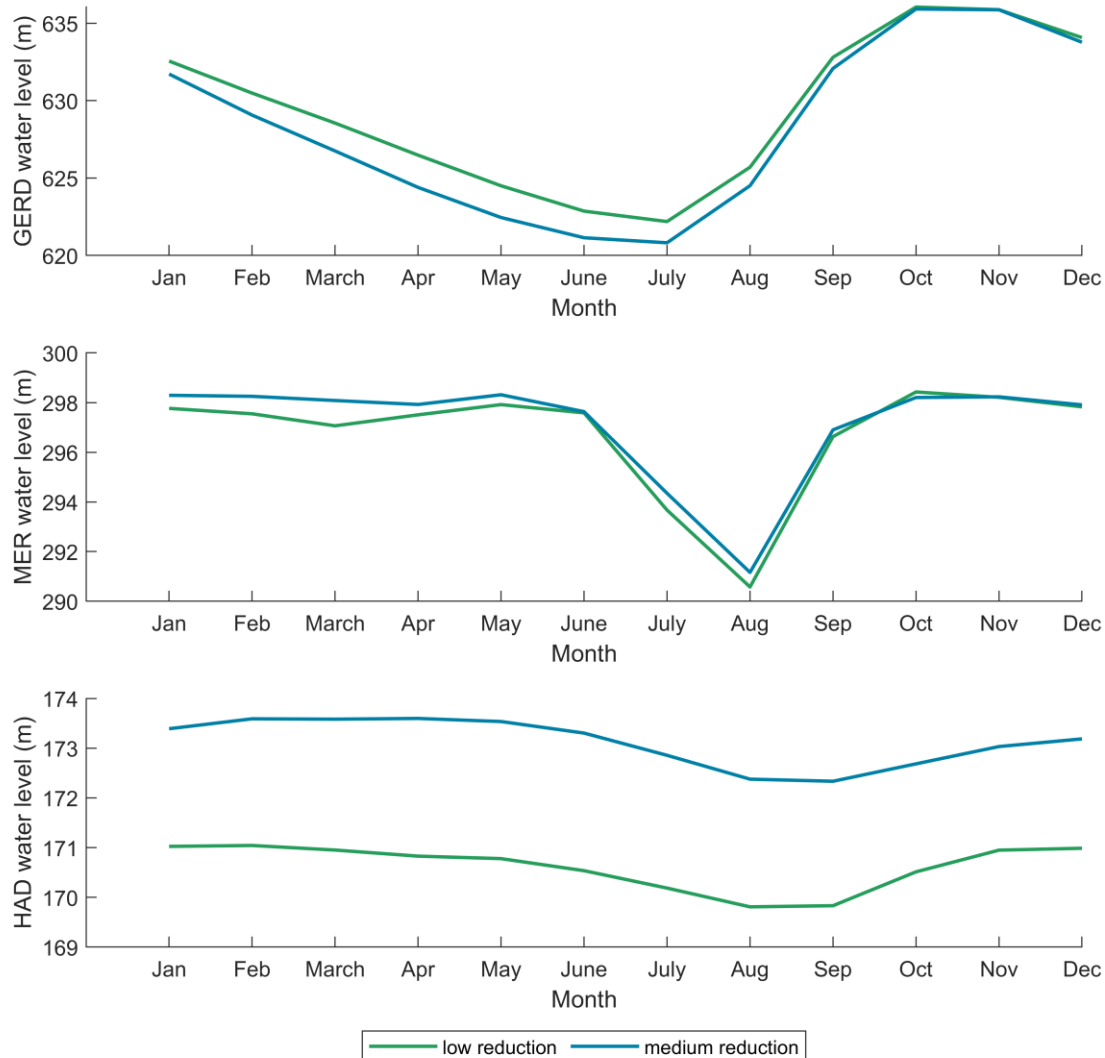


Figure 11 – GERD, MER and HAD water levels trajectory reported as annual means (on the left) and monthly mean (on the right) for the two selected solutions: low reduction (blue line) and medium reduction (green line).

To complement the information reported in Figure 9, we also computed for these two solutions the full list of evaluations indicators from D4.2. Results are shown in the parallel-axes plot of Figure 12. From the calculation of these indicators, we can note that although hydropower production is lower in the low-reduction solution (green line), the GERD's productions ($J^{E,GERD}$) are very similar in the two solutions, while Sudan ($J^{E,MER}$) and Egypt's productions ($J^{E,HAD}$) are reduced. It is interesting to note that the medium-reduction solution (blue line) is able to increase the hydroelectric production of the MER without decreasing the Sudanese irrigation deficit ($J^{Irr,Sudan}$). On the other hand, this solution is characterized by a slight increase in the Egyptian irrigation deficit ($J^{Irr,Egypt}$).

According to the sustainability indicator (Sandoval-Solis 2011) (J^S), that is an integration of performance criteria that capture the essential and desired sustainable characteristics of alternative portfolios

from the perspective of water users, the low-reduction solution is more sustainable than the medium-reduction one because this indicator is calculated with respect to the Egyptian irrigation deficits only. According to the water stress indicator (UNECE s.d.) (J^{WS}), both solutions have low performance, typical of countries with arid climates. This indicator indeed tracks how much freshwater is withdrawn by all economic activities, compared to the total renewable freshwater resources available, after taking into account environmental flows, calculated in this case at the basin scale. The solution with medium reductions performs slightly better because a larger reduction in downstream water demand increases water availability throughout the whole basin.

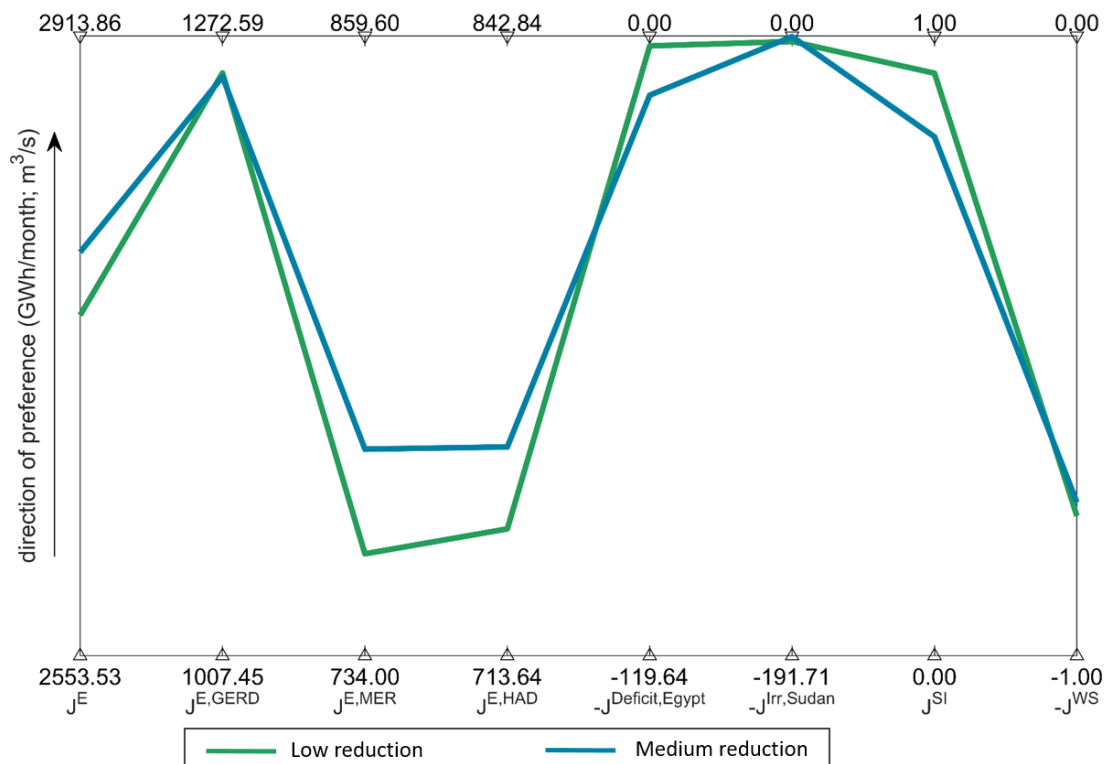


Figure 12 – Evaluation indicators for the Water Supply model computed for two representative solutions, one with for low reduction (green) and one for medium reduction (blue line).

After having analysed the results of these two selected solutions in the Water Supply model, we solved the Water Demand problem for the same two portfolios. The results obtained for the low water demand reduction alternative ($22.7 \text{ m}^3/\text{s}$) are illustrated in Figure 13, where the parallel-axes plot shows the volume allocated to the selected water demand reduction measures, e.g., reuse, groundwater, aquaponics and desalination plants, with the values at the top of the axes showing the maximum exploitation of the four measures. Moreover, a fifth axis indicates the feasibility of the desalination plants implemented in each solution. A solution is labelled as unfeasible if foresees one or more desalination plants with a capacity higher than $1,000,000 \text{ m}^3/\text{d}$. This value was chosen as threshold since there are no examples of bigger Reverse Osmosis plants in the reviewed literature. Only 5% of the obtained solutions are not feasible and coloured in grey in Figure 13.

Results show that reuse, groundwater and desalination reach similar maximum values, while aquaponics has a more limited range as we are only considering lettuce production for its implementation. To cultivate this crop, a total shift from traditional agriculture to aquaponics can reach 5.6% of the total water reduction considered in this alternative. The colours in Figure 13 are ordered according to the volumes allocated for desalination in each solution, where blue corresponds to low quantities and yellow to high ones. A clear trade-off between desalination and reuse and between desalination and groundwater can be identified by the diagonal lines between the axes, as low volumes of desalination correspond to high volumes of reuse and groundwater and vice versa.

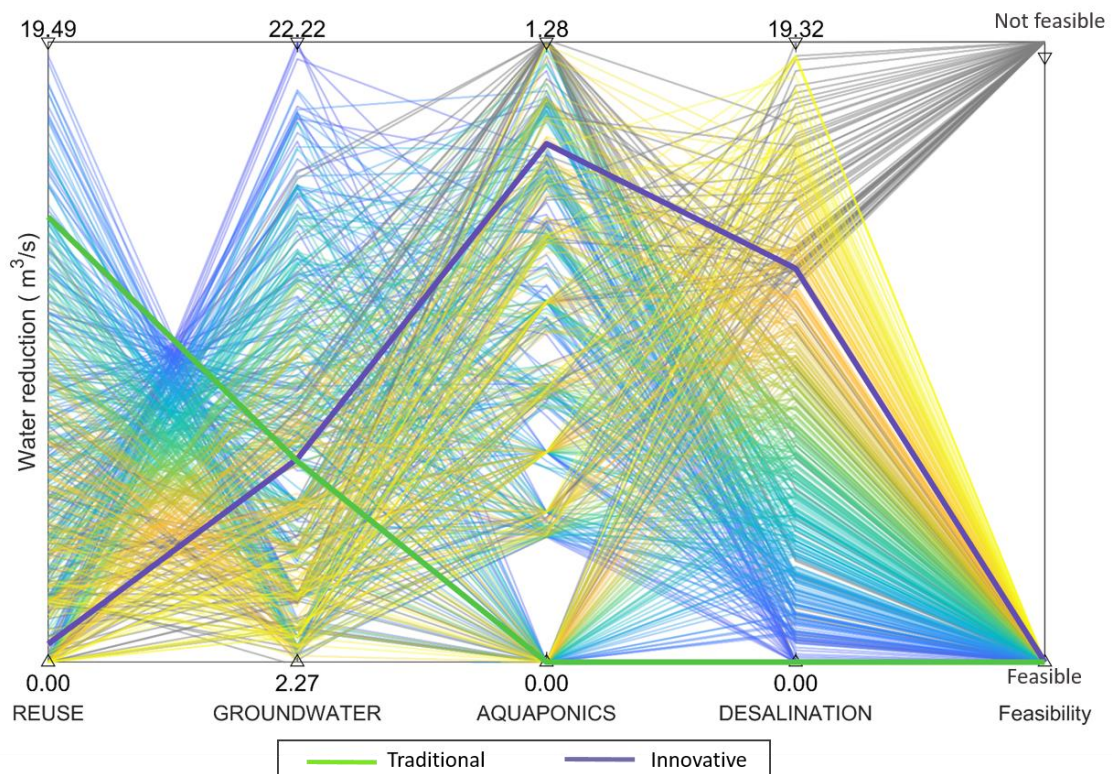


Figure 13 – Parallel plots of the Water Demand optimization for water reduction equals to 22.7 m³/s showing the volumes of water allocated to reuse, groundwater, aquaponics and desalination and the feasibility of the solution. The colours are assigned according to the desalination total capacity of every solution, with yellow associated with high values of desalination and blue to low one, while in grey are highlighted the unfeasible solutions. Two solutions are marked: one with high volumes of reuse and groundwater (*traditional* solution) in green and one with high volumes of aquaponics and desalination (*innovative* solution) in purple.

Two alternative water demand portfolios are selected in Figure 13 to explore in detail the spatial distributions of the water demand reduction measures in the eleven districts. The first solution, named as *innovative* and marked by a thick purple line in Figure 13, is characterised by a high use of desalination and aquaponics with a lower use of groundwater and reuse. This alternative bears high costs due to the setup of the facilities required and the large initial investments. It is considered advantageous as it uses straightforward and water-efficient technologies to reduce water demands. The second solution selected, named *traditional* and marked by a thick green line, is characterised by high volumes of water reuse and groundwater, and no contribution of aquaponics and

desalination. The traditional solution requires significantly lower costs, as the practices of water reuse from the agricultural drainage canals and groundwater pumping are already deeply exploited in the area, but it is expected to negatively impact on the ecosystem and water quality.

It is interesting to look at the distribution of the four measures in the eleven districts, reported in Figure 14. The behaviour shown is quite similar in the two solutions with the main difference being that reuse and desalination alternate in the Nile Delta. In both solutions, there is a large use of groundwater in the first five districts, all of which are located along the river Valley only and outside the Delta to limit the risks of sea water intrusion. Unlike the other measures, the distribution of aquaponics does not seem to follow any specific pattern and the algorithm optimises its use both inside and outside the Delta.

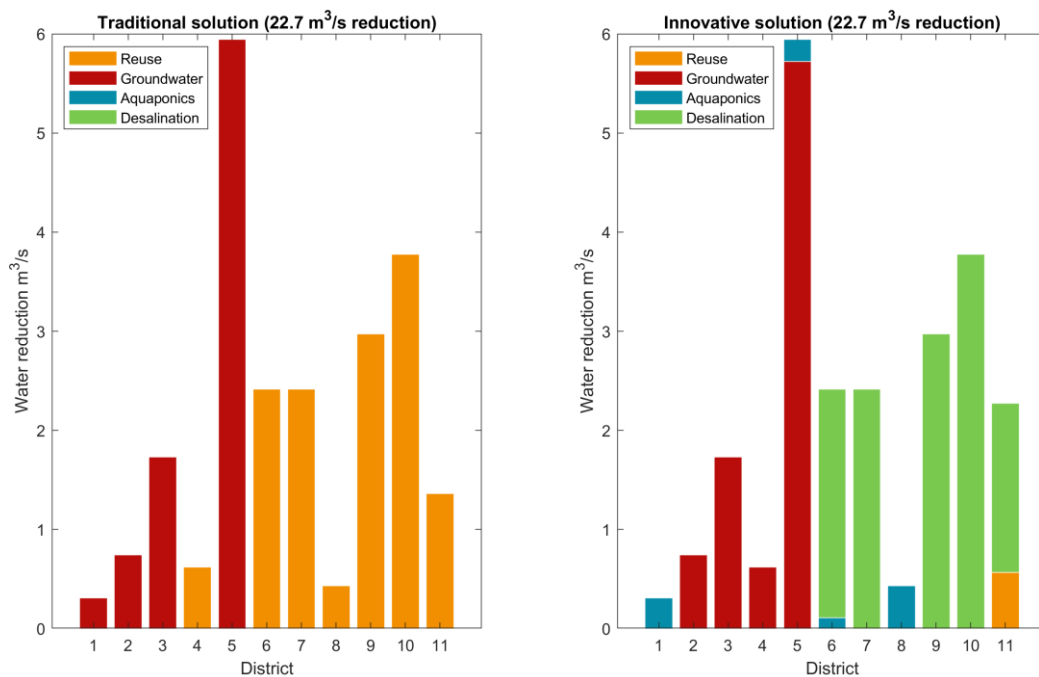


Figure 14 – Spatial distribution of water demand reduction measures for the *traditional* solution (on the left) and *innovative* solution (on the right). The districts are reported on the horizontal axis with numbers from 1 to 11: (1) Asfoun, (2) Kelabia, (3) West Naga, (4) East Naga, (5) Ibrahimia, (6) Tawfiki, (7) Ismailia (8) Sharkawia, (9) Menufia, (10) Beheria, (11) Nasseri.

Figure 15 shows the results obtained for the optimization of the medium water reduction solution (92.5 m³/s). The results present a similar pattern to the one in Figure 13, where high volumes of desalination correspond to low volumes of groundwater and reuse. The main difference lies in the larger volumes of water allocated to reuse, groundwater and desalination. The maximum water reduction achievable by implementing aquaponics is still 1.28 m³/s, which corresponds to only 1.2% of the total desired water reduction. If we look at the desalinator capacities obtained in this optimisation, only 10% of the solutions have a capacity lower than 1,000,000 m³/d and would be considered feasible with existing technologies. It is interesting to notice that the increase in the demand reduction target makes it essential to consider solutions with a diverse portfolio of measures.

Favouring reuse and groundwater may lead to exceed the legal limits allowed for these measures and to negative environmental consequences, while implementing only desalination may result in solutions that are not feasible due to technological limitations.

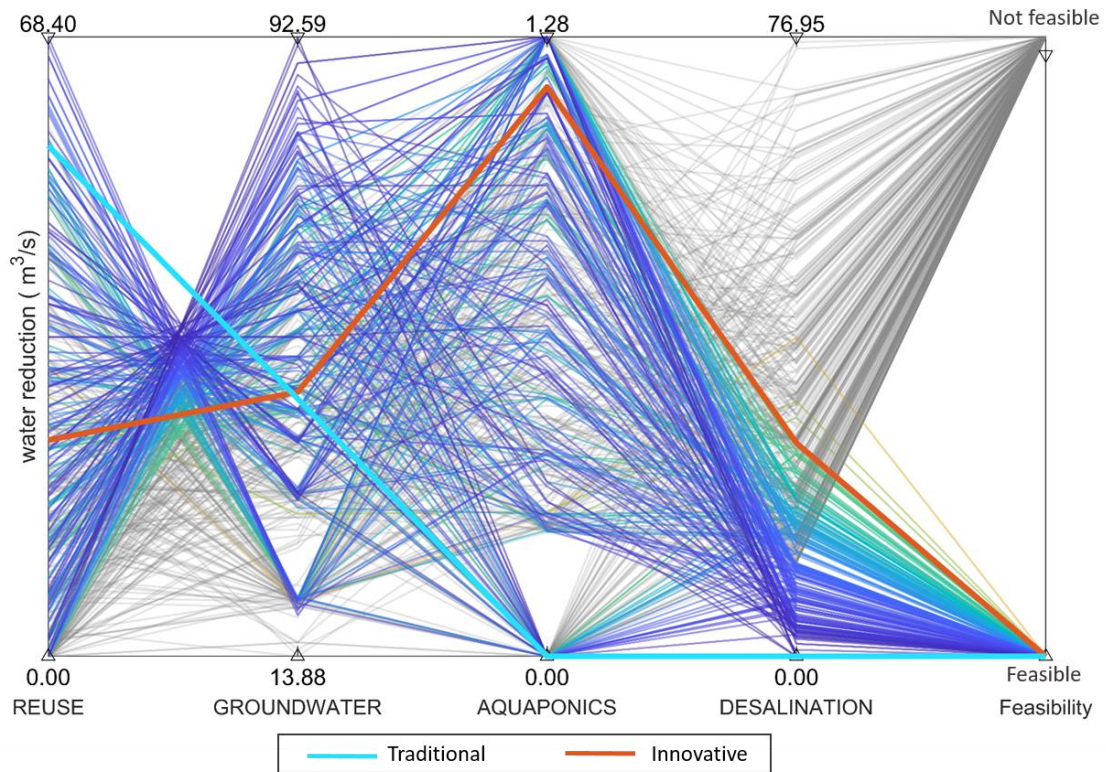


Figure 15 – Parallel plots of the Water Demand optimization for water reduction equals to 92.8 m³/s showing the volumes of water allocated to reuse, groundwater, aquaponics and desalination and the feasibility of the solution. The colours are assigned according to the desalination total capacity of every solution, with yellow associated with high values of desalination and blue to low one, while in grey are highlighted the unfeasible solutions. Two solutions are marked: one with high volumes of reuse and groundwater (*traditional* solution) in light blue and one with high volumes of aquaponics and desalination (*innovative* solution) in orange.

Similarly to the previous experiments, two solutions are selected among the feasible ones in Figure 15, again one characterized by high volumes of desalination and aquaponics (*innovative*) and one exploiting only reuse and groundwater (*traditional*). The distribution of the measures in the districts, reported in Figure 16, resembles the one of the low reduction alternative, where groundwater is mainly used in the Nile Valley and reuse and desalination in the Delta. In these two solutions, we observe how the algorithm also places groundwater within the Delta in reduced quantities. As the reduction volume increases, it becomes necessary to extract groundwater also in the Delta.

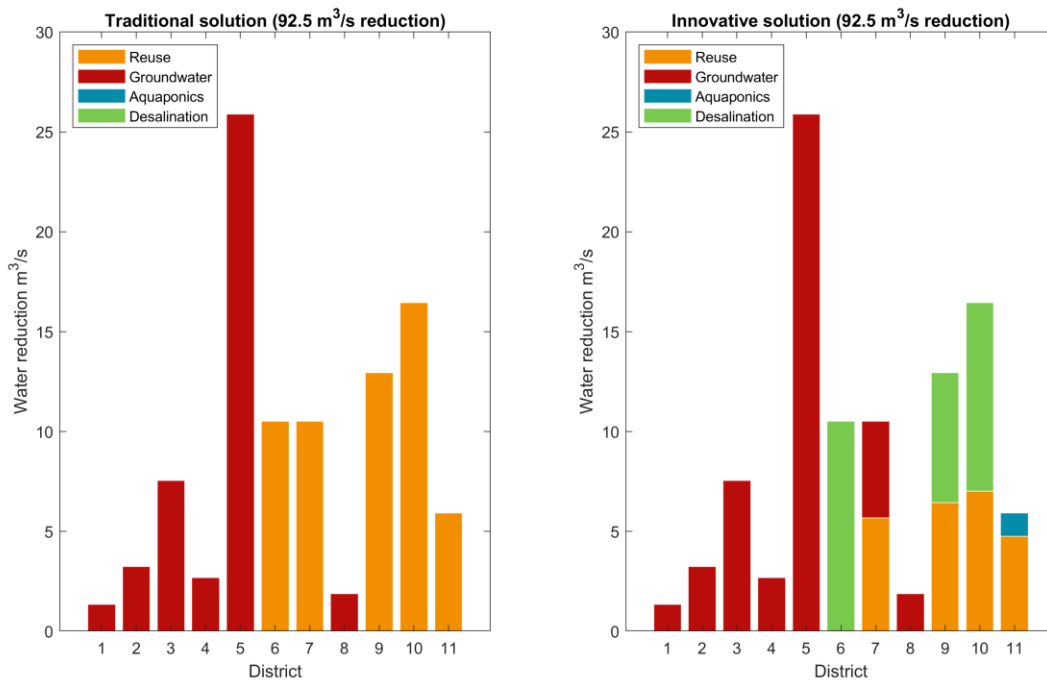


Figure 16 – Spatial distribution of water demand reduction measures for the *traditional* solution (on the left) and *innovative* solution (on the right). The districts are reported on the horizontal axis with numbers from 1 to 11: (1) Asfoun, (2) Kelabia, (3) West Naga, (4) East Naga, (5) Ibrahimia, (6) Tawfiki, (7) Ismaila (8) Sharkawia, (9) Menufia, (10) Beheria, (11) Nasserri.

The analysis of the full set of evaluation indicators for the Water Demand model is shown in Figure 17. The alternatives are represented as horizontal lines crossing sixteen axes representing the values of each evaluation indicator.

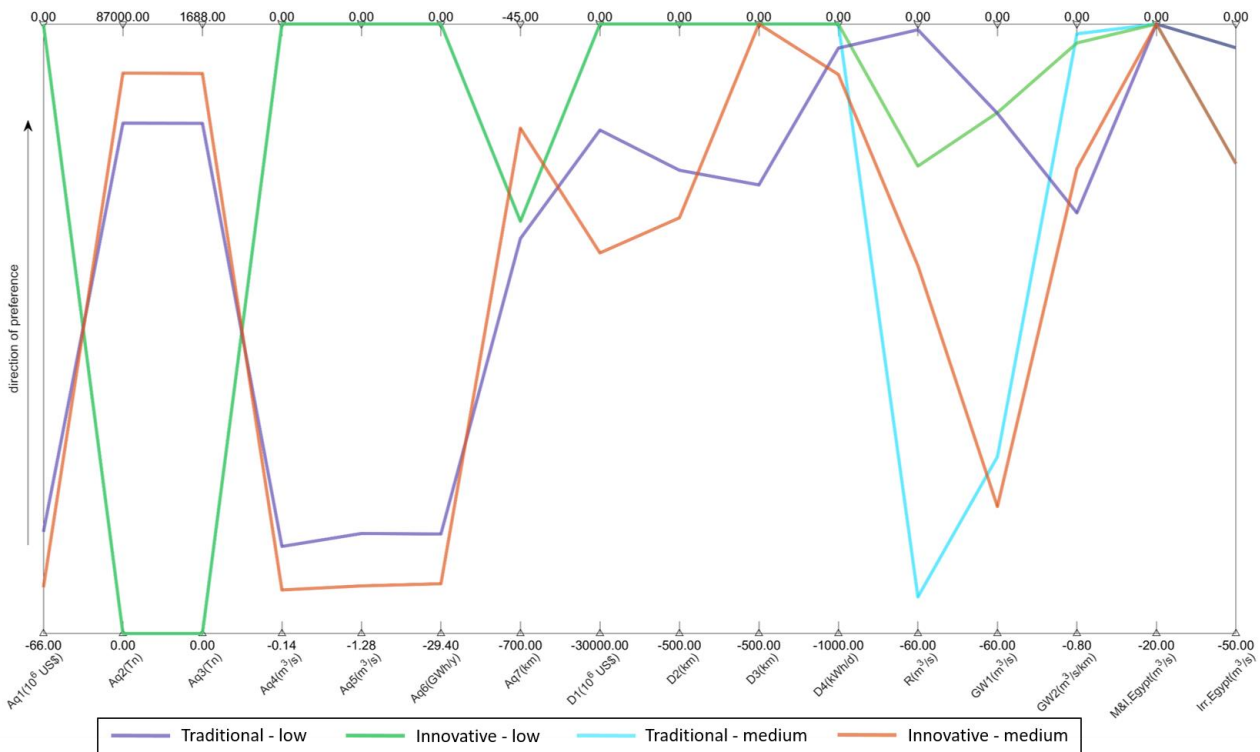


Figure 17 – Evaluation indicators for the Water Demand model computed for four representative solutions, two selected in the low reduction optimization (green and violet) and two selected in the medium reduction optimization (light blue and orange).

Results show that the two traditional solutions (light blue and green lines) are partially overlapping, as these do not include the implementation of aquaponics or desal and, as a consequence, the indicators referring to these two measures assume the same values for both measures. The two innovative solutions, on the other hand, involve the implementation of both aquaponics and desalination technologies. The innovative-medium solution foresees a shift from traditional agriculture to aquaponics of 90% of the total lettuce revenue of the country, while the innovative-low solution of 84%. Consequently, the innovative-medium solution requires higher costs for the implementation of the aquaponics system (Aq1), higher water consumption (Aq5) and electricity consumption (Aq6); on the other hand, it can produce larger quantities of lettuce (Aq2) and fish (Aq3) and has higher water savings compared to traditional agriculture (Aq4). Furthermore, in this solution, the aquaponics systems are located closer to Cairo (Aq7), thus enhancing the robustness against pandemic risks with respect to the existing distribution of traditional lettuce production. For the innovative-low solution, however, this indicator worsens slightly compared to the current situation, as the solution involves the placement of aquaponics in some districts far from the Cairo.

The innovative-medium solution has a higher total desalination capacity than the innovative-low solution. It foresees three desalination plants between 500,000 and 900,000 m³/d for an investment of 375,000 US\$. Conversely, the low innovative two desalination plants of medium-high capacity, one of 400,000 m³/d, and the second one of 650,000 m³/d. The investment required by these two plants for each year would amount to 174,000 US\$. In addition to having higher CAPEX and OPEX

for desalination (D1), the medium reduction solution consumes more energy (D2) and has higher water transport costs from shore to the district (D3) than the low reduction solution, while water transport costs from one district to another (D4) are lower for the medium reduction alternative since it does not have any desalinated water transport between districts.

The solutions for medium reductions use groundwater and reuse to a greater extent and are therefore characterised by higher values of the indicators referring to them (R, GW1 and GW2). Finally, the deficit indicator for the municipal and industrial sectors (M&I, Egypt) is zero for all solutions. Since these sectors have priority over the irrigation one, deficits are generated only in cases of extreme drought. In the two innovative solutions, part of the industrial and municipal deficit is met by desalinated water and water savings from aquaponics. According to the prioritisation rule, water from desalination and aquaponics is used to meet industrial and municipal demand and is only used for agricultural demand if the total volume of water obtained through these two measures exceeds urban and industrial demand. As far as the irrigational deficit of Egypt (Irr,Egypt), the two low-reduction solutions have lower deficit values than the medium-reduction solutions.

5.2 THE ROLE OF INTERNATIONAL COOPERATION

The results discussed in the previous section assume a scenario of full cooperation under which Ethiopia, Sudan and Egypt agree to collaboratively operate their water infrastructures for maximizing basin-level benefits. In order to explore the role of international cooperation, we run a second experiment where the Water Supply model is optimising the hydroelectric production of GERD separately from the rest of the system, thus assuming no international cooperation between Ethiopia and the downstream countries.

The results of this experiment are shown in the parallel-axes of Figure 18, where they are compared with the solutions under full cooperation. In the non-cooperative scenario (yellow lines), GERD is not surprisingly able to produce more hydropower than in the cooperation scenario (blue lines). The country that experiences more losses is Sudan, which, being immediately downstream of the GERD, would suffer negative impacts in terms of both hydroelectric production and agricultural deficit if the GERD was operated without considering the downstream system. Egyptian hydropower production is less affected than that of Sudan, and it continues to achieve production in the same range of the cooperative optimisation, although there is a lowering of the maximum production. Even looking at the Egyptian irrigation deficit, the new optimisation produces similar levels to the previous one. This result is however attributed to the introduction of water demand reductions. Looking at these results, the scenario without cooperation emerges as dominated when looking at the river-basin benefit as also captured by SDG indicator 6.5.2 (Indicator | SDG 6 Data. s.d.), and it is particularly not sustainable for Sudan. This is why we hope that the three countries will move towards an arrangement for water cooperation.

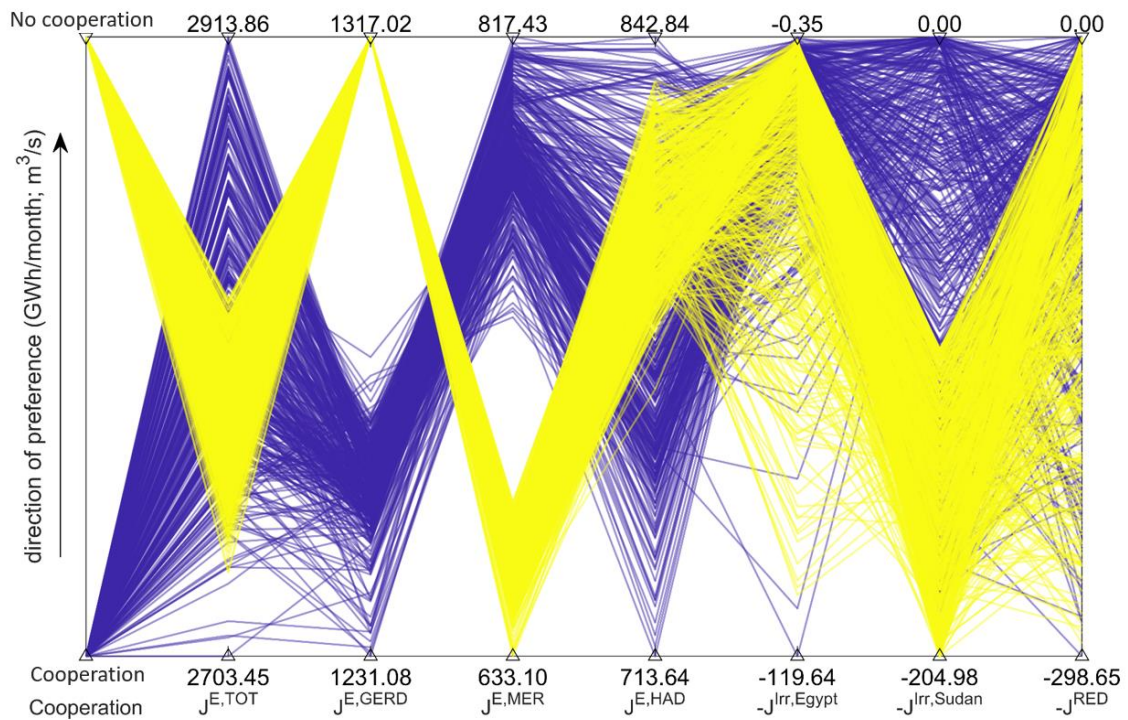


Figure 18 – Parallel plot for the optimization of the Water Supply model under historical condition for cooperative scenario (blue lines) and non-cooperative scenario (yellow lines). For every solution is reported the hydropower production at the basin scale ($J^{E,TOT}$), in Ethiopia ($J^{E,GERD}$), Sudan ($J^{E,MER}$) and Egypt ($J^{E,HAD}$), Egypt irrigation deficit ($-J^{Irr,Egypt}$), Sudan irrigation deficit ($-J^{Irr,Sudan}$) and water reductions below HAD ($-J^{RED}$).

5.3 FUTURE CONDITIONS

The optimization of the Water Supply and Water Demand models are then repeated with the projected scenarios of water availability and demand illustrated in Section 4. The new results obtained for the Water Supply model are shown in Figure 19 in terms of hydropower production at the basin scale and for the three dams GERD, MER and HAD, the irrigation deficits of Sudan and Egypt and the water demand reductions below HAD. Each solution is represented as a horizontal line crossing the seven vertical axes at the value of the corresponding performance, with the optimal solution that would be represented by a line crossing all axes at the top. As in previous figure, we can notice that the main trade-off is between hydropower production and irrigation demand.

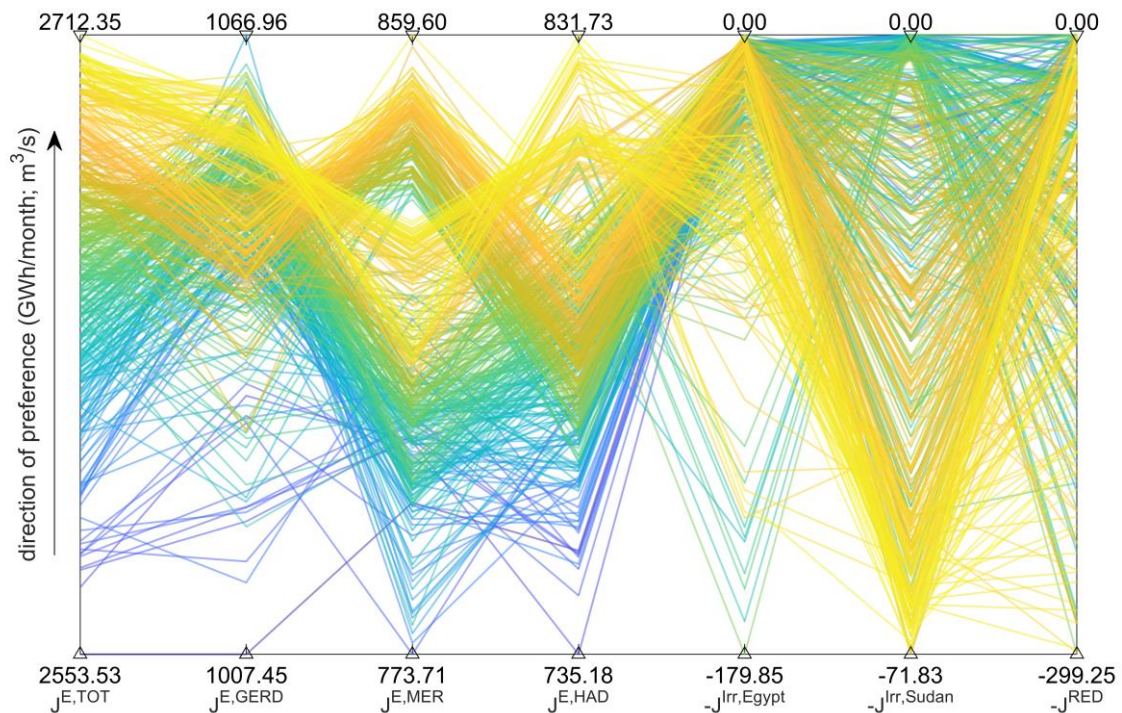


Figure 19 – Parallel plots of the Water Supply optimization showing hydropower production at the basin scale ($J^{E,TOT}$), in Ethiopia ($J^{E,GERD}$), Sudan ($J^{E,MER}$) and Egypt ($J^{E,HAD}$), Egypt irrigation deficit ($-J^{Irr,Egypt}$), Sudan irrigation deficit ($-J^{Irr,Sudan}$) and irrigation reductions below HAD ($-J^{RED}$). The colour are assigned according to the level of energy produced at the basin scale ($J^{E,TOT}$), where yellow line corresponds to high energy productions and blue lines to low one.

Compared to the results obtained with the historical optimisation (s. Figure 9), the hydropower production on a basin scale is greatly reduced: while under the historical scenario it is possible to achieve production levels up to 2900 GWh/month, in the future the optimized portfolios do not exceed 2700 GWh/month. Looking at the individual hydropower production of the three dams, it can be observed that the losses in hydropower production are mainly due to a reduction in GERD's generation, while MER's production increases and that of HAD maintains levels similar at the historical optimization. The reduction in energy production in the GERD can be attributed to the decrease in the Blue Nile inflow, while the lower water demand in Sudan, achieved through the reallocation of crops, ensures that more water is available for hydropower production in Sudan and Egypt.

The introduction of measures to reduce demand below HAD can alleviate the conflict between the hydropower and irrigation sectors. Figure 20 shows the hydropower production against the aggregate deficit of Sudan and Egypt, where the colour of the solutions is given by the intensity of the water demand reduction. The two solutions marked in Figure 20 as triangles are selected for further analysis. They both attain a low deficit and implement demand reductions equal to 50.9 m³/s and 98.5 m³/s, respectively. The higher demand reduction allows increasing the total hydroelectric production by approximately 50 GWh/month.

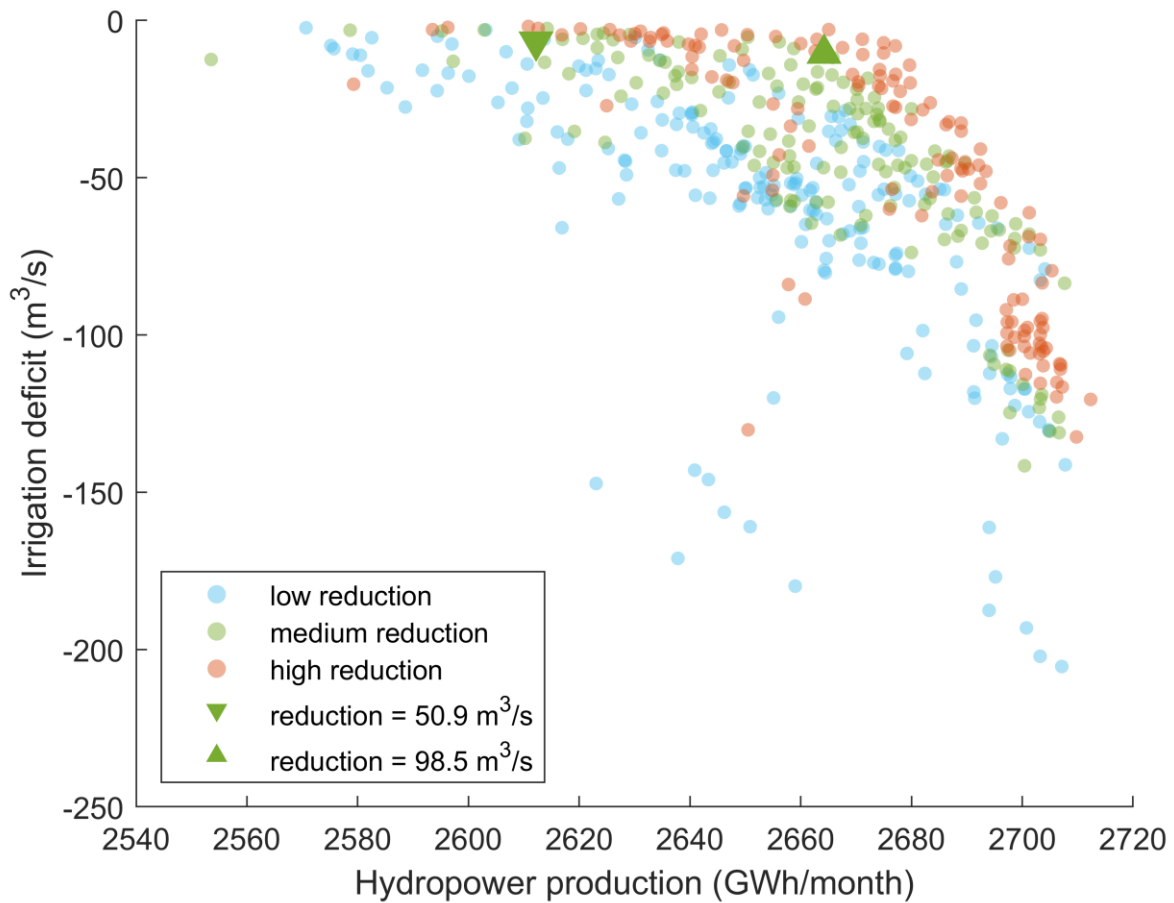


Figure 20 – Scatter plot representing the total hydropower produced at the basin scale against the aggregated irrigation deficit of Sudan and Egypt. To each solution is associated a colour representing the volume of water reduction: blue for reduction lower than 25 m³/s, green for reduction between 25 to 100 m³/s and red for reductions higher than 100 m³/s. Two solutions are represented as triangles one for 50.9 m³/s of water reduction and one for 98.5 m³/s. Two solutions are marked with triangles, one for 50.9 m³/s of water reduction and one for 98.5 m³/s.

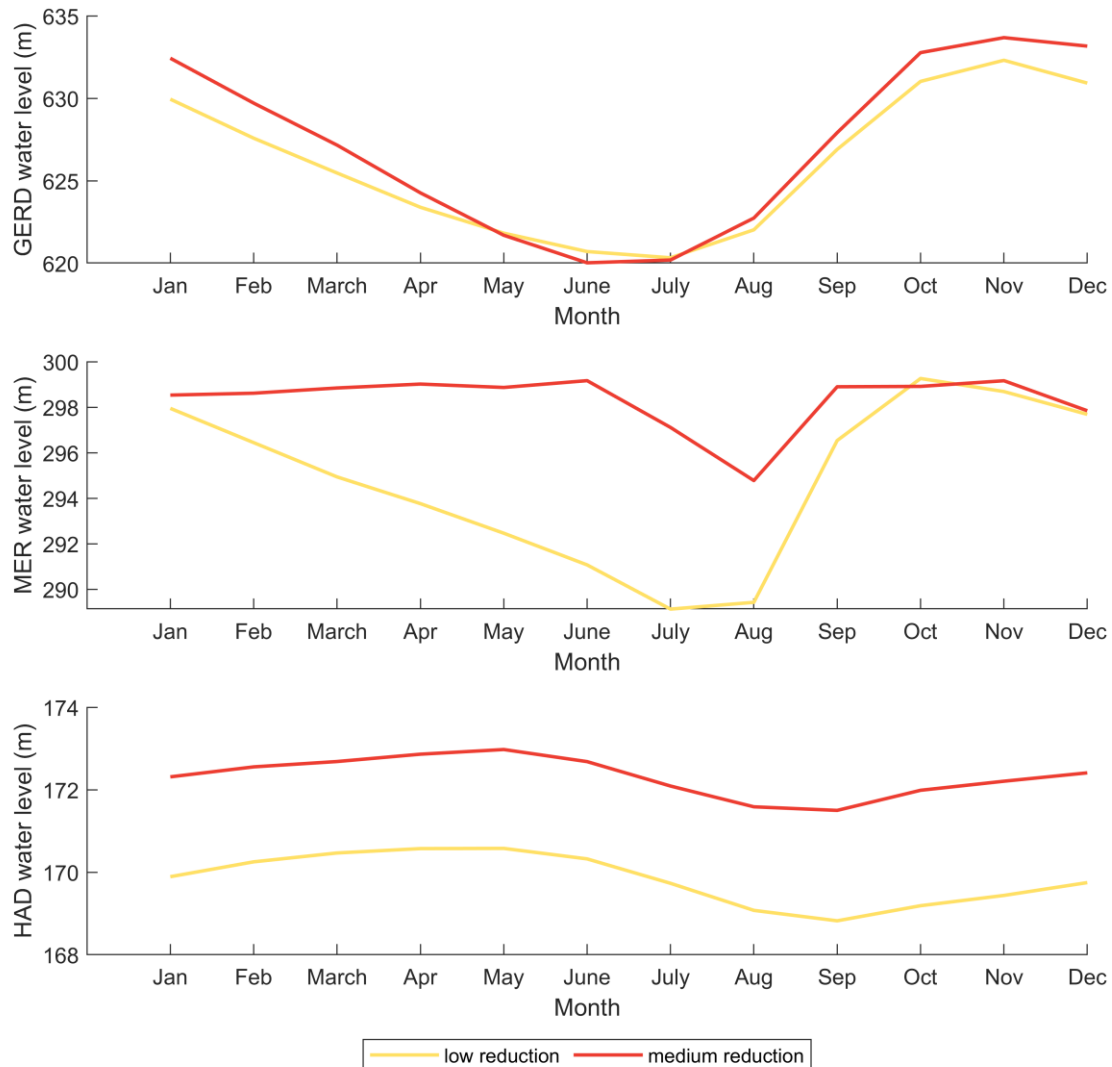


Figure 21 – GERD, MER and HAD water levels trajectory reported as annual means (on the left) and monthly mean (on the right) for the two selected solutions: low reduction (yellow line) and medium reduction (red line).

For the two selected solutions, the simulated level of the three reservoirs can be observed (Figure 21). Similarly to what observed under historical conditions (Figure 11), the solutions attaining a higher hydropower production (red line) tends to maintain higher water levels, while the solution with the smaller deficit (yellow line) has lower levels. The level of the GERD reservoir is similar for the two alternatives, as it is less influenced by what happens downstream. In contrast to what observed in the previous subsection, both MER and HAD are influenced by the irrigation requirements, as indicated by the different trajectories of the two reservoirs for the two solutions. This indicates that climate change will exacerbate the trade-offs in the basin, making energy production in Sudan more sensitive to the water consumed by the Sudanese agricultural sector.

The evaluation indicators related to the Water Supply model are computed for these two solutions and plotted in Figure 22 as yellow and red lines, which are compared against the historical ones represented by blue and green lines. As anticipated, we can easily notice that the hydropower produced for the future scenario at the basin scale ($J^{E,TOT}$) is much lower compared to the two historical solutions. Notably, looking at the hydropower production in the three dams, only the generation of the GERD ($J^{E,GERD}$) is lower in the future, whereas the productions for MER ($J^{E,MER}$) and HAD ($J^{E,HAD}$) are actually higher. The levels of deficits of these two solutions are instead similar to the deficits obtained in the previous optimization. The solution for medium reductions (red line) has a higher deficit for Egypt compared to the low reduction solution (yellow line), while both solutions have the same level of Sudanese deficit. It is interesting to notice that the solution with higher water reductions can increase the energy produced in Sudan without decreasing the irrigation deficit of the country.

As before, the solution with medium water reduction optimized over future scenario performs worse according to the sustainable index compared to the low reduction, as this solution has a higher Egyptian water deficit. On the other hand, it performs better according to the water stress index. Although there will be a decrease in water availability in the future due to climate change, the performance of the water stress indicator does not deteriorate compared to historical solutions. This can be attributed to the decrease of Sudan water demand in the assumed scenario, which counterbalances the future reduction in Nile runoff.

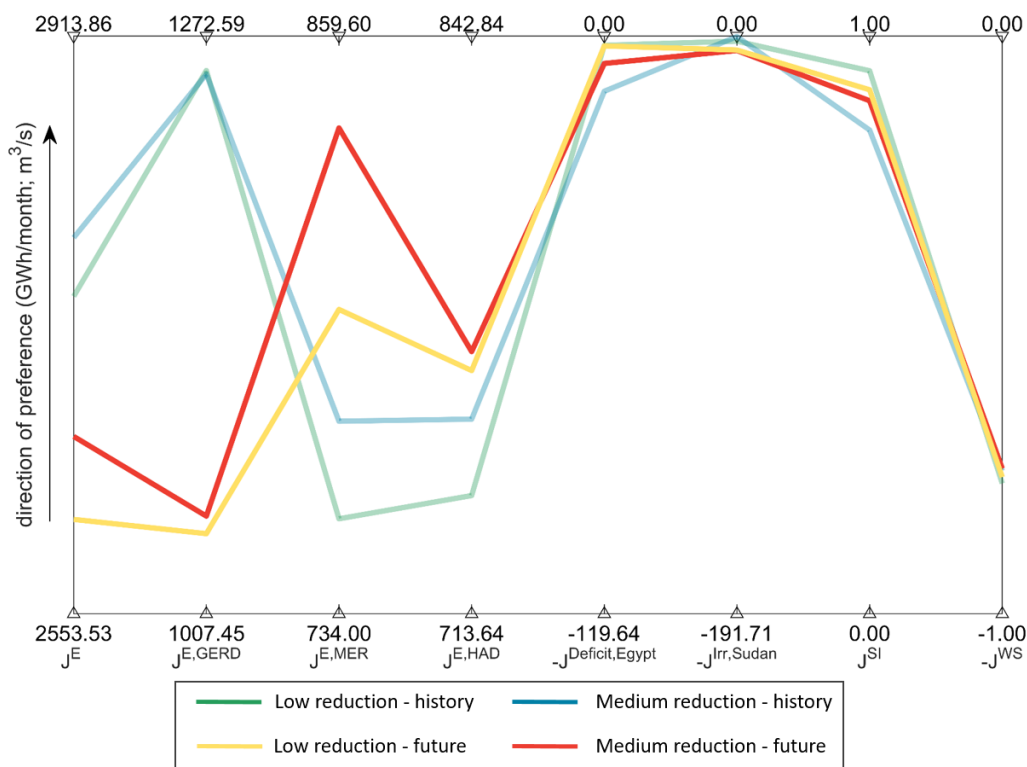
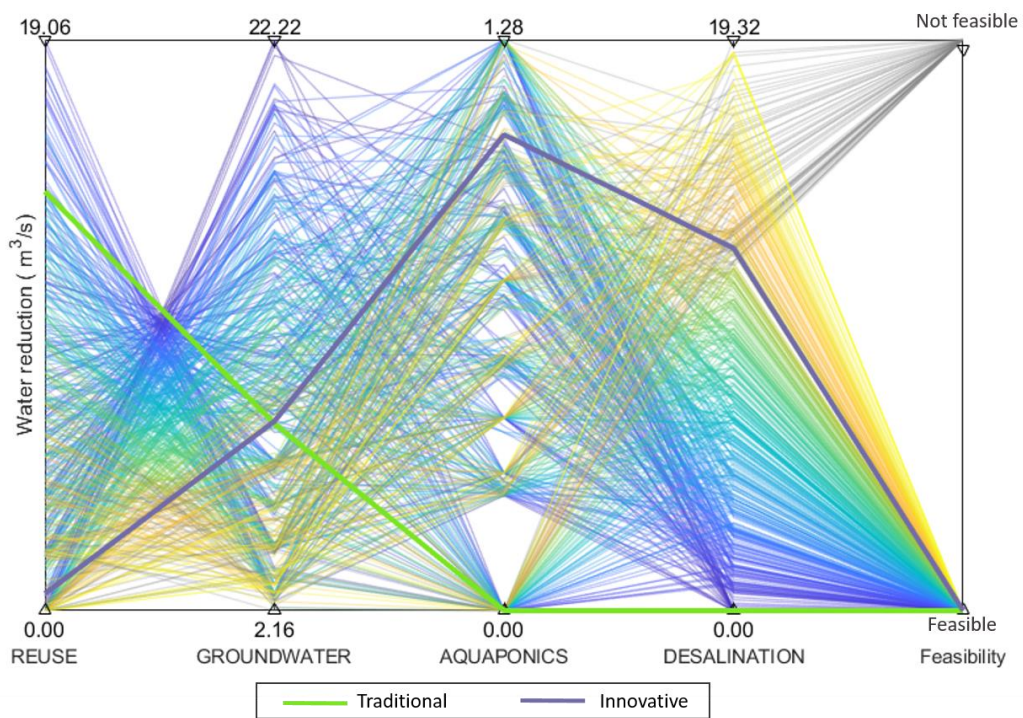


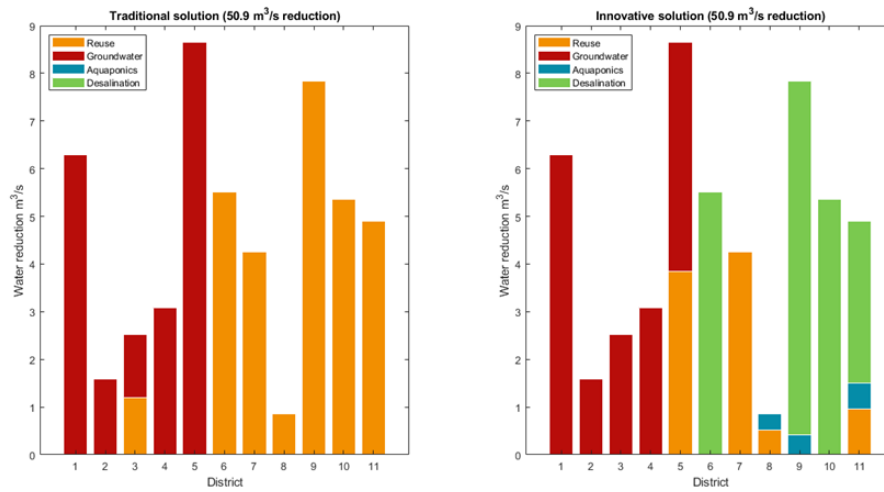
Figure 22 – Evaluation indicators for the Water Supply model computed for four representative solutions, two for the historical optimization (green and blue) and two for the future optimization (yellow and red).

The two selected solutions are finally optimized using the Water Demand model. The results for the optimization of the low reduction solution are shown in Figure 23a, where the trade-offs are similar to the historical conditions with a first set of solutions having high desalination volumes and low groundwater and reuse volumes and a second set of solutions relying mostly on reuse and groundwater only. In this optimization under future conditions, 70% of the solutions have desalination plants with feasible capacity, while the maximum water reduction achievable thanks to aquaponics is equivalent to the 2.5% of the total water reduction target.

Two solutions are then selected among the one displayed in Figure 23a: one employs only reuse and groundwater (*traditional*, see thick green line) and one that also employs desalination and aquaponics (*innovative*, see thick violet line). Figure 23b shows the distribution of the four measures in the eleven districts for the selected alternatives. As it occurred for the solutions selected for the historical scenario, groundwater is used only in the Nile Valley (i.e. from the first district until the fifth district), while desalination is only used in the Delta. Reuse is also mostly employed in the Delta.



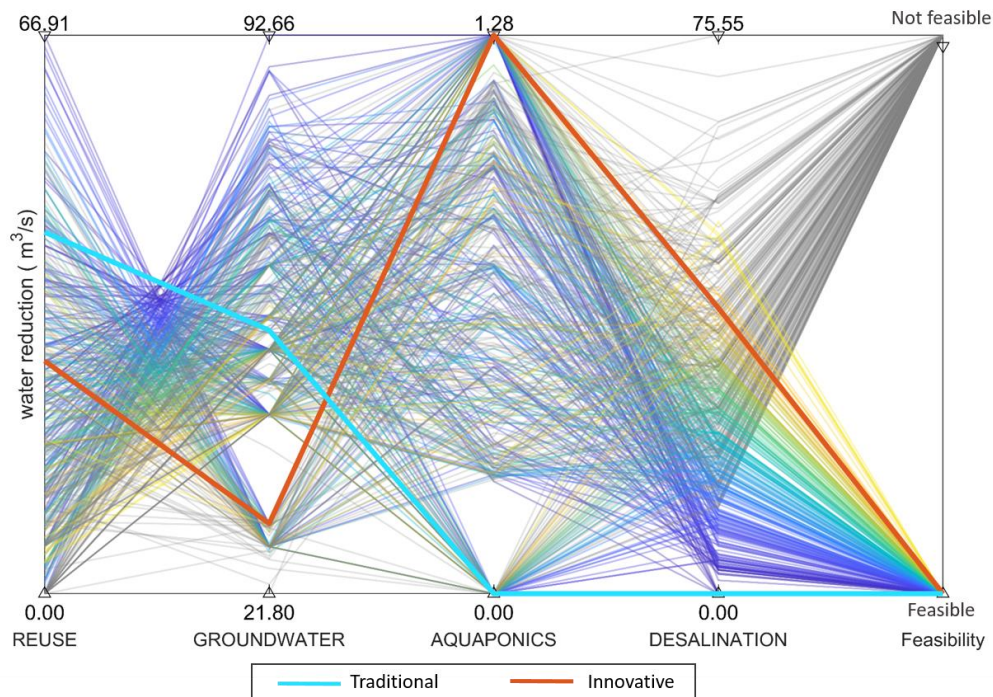
(a)



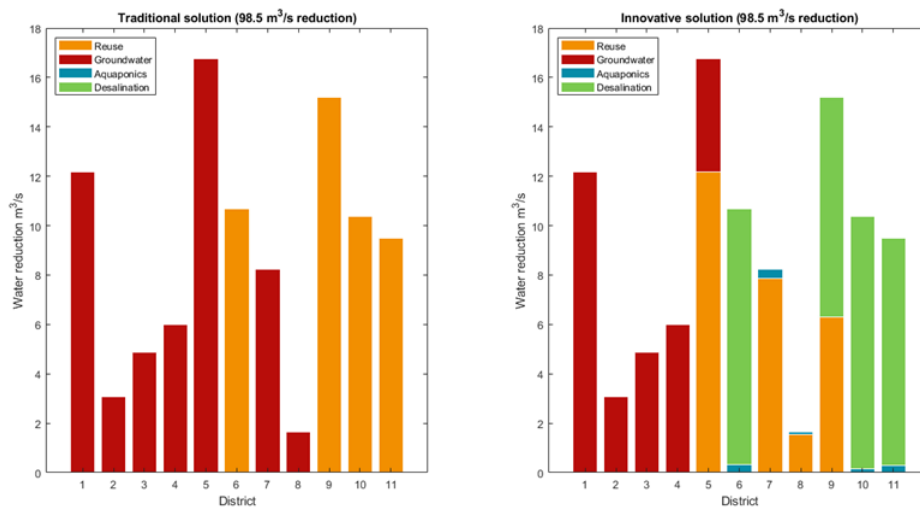
(b)

Figure 23 – (a) Parallel plots of the Water Demand optimization for water reduction equals to 50.9 m³/s showing the volumes of water allocated to reuse, groundwater, aquaponics and desalination and the feasibility of the solution. The colours are assigned according to the desalination total capacity of every solution, with yellow associated with high values of desalination and blue to low one, while in grey are highlighted the unfeasible solutions. Two solutions are highlighted one with high volumes of reuse and groundwater (*traditional* solution) in light green and one with high volumes of aquaponics and desalination (*innovative* solution) in purple. (b) Spatial distribution of water demand reduction measures for the *traditional* solution (on the left) and *innovative* solution (on the right). The districts are reported on the horizontal axis with numbers from 1 to 11: (1) Asfoun, (2) Kelabia, (3) West Naga, (4) East Naga, (5) Ibrahimia, (6) Tawfiki, (7) Ismaila (8) Sharkawia, (9) Menufia, (10) Beheria, (11) Nasseri.

The results obtained with the Water Demand model for the portfolio of medium reduction under future conditions are represented in Figure 24a. Again, two solution, *traditional* and *innovative*, are selected and marked in thick light blue and orange lines in Figure 24a. The allocation of water demand measurements in the districts (Figure 24b) still shows how the portfolios design prefers to place groundwater in the districts outside the Delta, and reuse and desalination in the Delta. In the traditional solution, groundwater is also used in the sixth and seventh districts that are both in the Delta because the intensity of water reduction targets increases.



(a)



(b)

Figure 24 – (a) Parallel plots of the Water Demand optimization for water reduction equals to $98.5 \text{ m}^3/\text{s}$ showing the volumes of water allocated to reuse, groundwater, aquaponics and desalination and the feasibility of the solution. The colours are assigned according to the desalination total capacity of every solution, with yellow associated with high values of desalination and blue to low one, while in grey are highlighted the unfeasible solutions. Two solutions are highlighted one with high volumes of reuse and groundwater (*traditional* solution) in light blue and one with high volumes of aquaponics and desalination (*innovative* solution) in orange. (b) Spatial distribution of water demand reduction measures for the *traditional* solution (on the left) and *innovative* solution (on the right). The districts are reported on the horizontal axis with numbers from 1 to 11: (1) Asfoun, (2) Kelabia, (3) West Naga, (4) East Naga, (5) Ibrahimia, (6) Tawfiki, (7) Ismailia (8) Sharkawia, (9) Menufia, (10) Beheria, (11) Nasseri.

Finally, the evaluation indicators for the Water Demand model are computed for these two solutions and the one previously selected for the low water reduction optimization. The values obtained are reported in a parallel-axes plot (Figure 25), where the two traditional solutions (green and light blue lines) are partially overlapping. Both traditional solutions do not involve the development of desalination and aquaponics, and therefore assume the same values for the indicators referring to them. The two innovative solutions (purple and orange lines) are also partially overlapping as both involve a total conversion of the lettuce produced of Egypt from traditional farming to aquaponics. The two solutions involve an investment of 66,000 US\$ (Aq1) for the implementation of one or more aquaponics systems capable of producing 87000 Tn of lettuce (Aq2) and 1688 Tn of fish (Aq3) in one year. A system of this capacity consumes 1.28 m³/s of water (Aq5) and 29.40 GWh/year of energy (Aq6). Both solutions improve the positioning of the lettuce cultures (Aq7) compared to the current situation, given by the traditional solutions. However, the two solutions have different desalination efforts, with larger volumes of water being desalinated for the medium reduction solution (orange line). This solution involves the construction of four desalination plants, all of large capacities, in districts Tawfiki, Menufia, Beheria and Nasserri without the exchange of desalinated water with other districts. The total investment for this implementation is 530,000 \$/y (D1) and involves an energy consumption of 120 kWh/d (J^{D4}). The proxy cost of transporting water from the sea to the districts is 209 km (D2), while the proxy cost of distributing water is zero as there is no transport of desalinated water outside the districts where it is produced. The innovative solution with low water demand reductions (purple line), on the other hand, involves the construction of three desalination plants, two medium-sized, in districts Tawfiki and Menufia, and one of large capacity in district Nasserri, which also supplies water to district Beheria. This implementation requires an investment of 300,000 US\$/y and an energy consumption of 65 kWh/d, both values are lower compared to the previous implementation given the smaller installed capacity of this solution. The proxy cost of water supply is also lower compared to the other innovative solution, given the smaller number of plants, while the proxy costs of water distribution are higher due to the interconnections for the exchange of desalinated water from district Beheria to district Nasserri.

Looking at the evaluation criterion for groundwater and reuse (R, GW1, GW2) the innovative solution for low reduction has the lowest values for all the indicators while the traditional solution for medium reduction (blue line) has the highest one. As in the historical optimization, the deficits for the industrial and municipal sectors are null since they have the priority over the irrigation sector, while the irrigation deficit is higher for the two solutions for medium reduction. Again, water contributions from desalination and aquaponics are fully used for municipal and industrial demand, as formulated in the prioritisation rule. Reuse and groundwater, on the other hand, are used exclusively for irrigation demand.

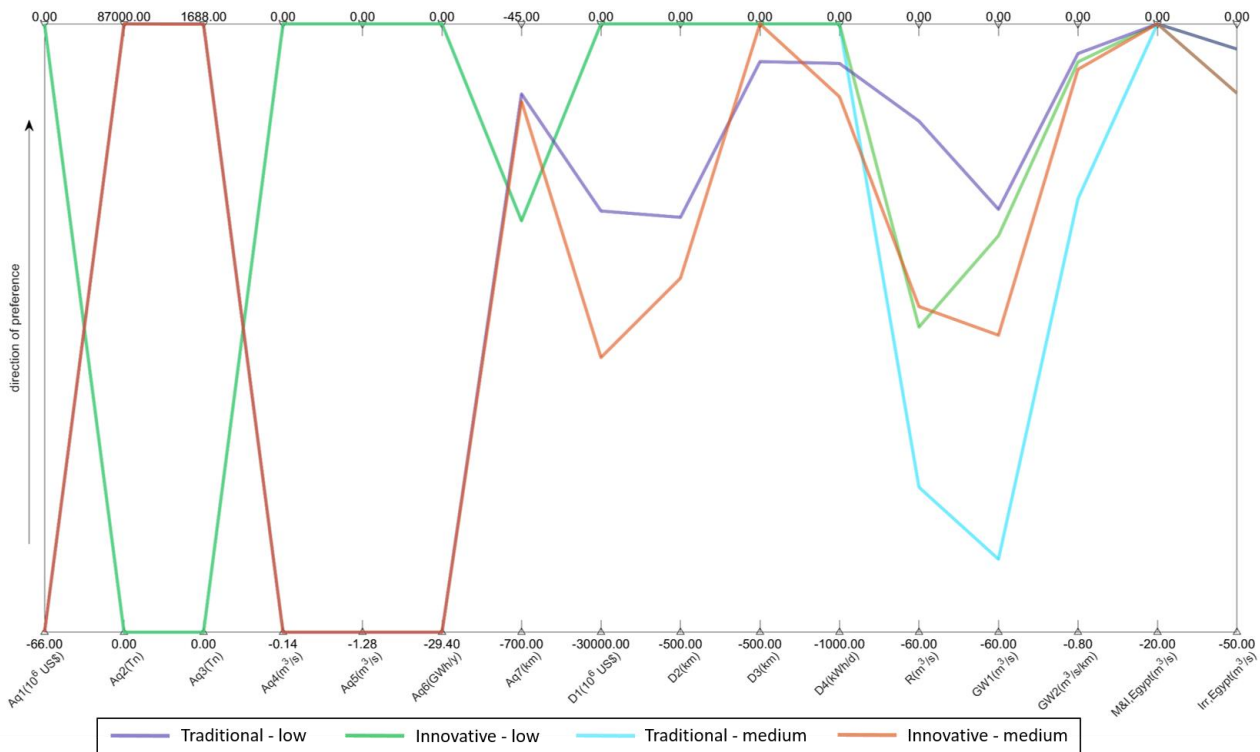


Figure 25 – Evaluation indicators for the Water Demand model computed for four representative solutions, two selected in the low reduction optimization (green and violet) and two selected in the medium reduction optimization (light blue and orange).

The last experiment carried out is the optimisation of the Water Supply model for the future scenario, according to non-cooperative assumption. In this case, as before, Ethiopia is the only country to benefit from this optimisation. Looking at Figure 26, where the new optimisation (yellow lines) is compared to the previous one (blue lines), GERD hydropower production is higher in the non-cooperative scenario, while the different downstream sectors are penalised. Egyptian hydropower production is also damaged, unlike in the historical optimisation (Figure 18) where it was possible to achieve good levels of hydropower for HAD even without a coordinated policy. The Egyptian irrigation sector is the only one not affected by this policy, thanks to the introduction of water demand reduction measures. These results show that cooperation between states is necessary, especially in view of climate change that will lead to worsening drought conditions in this basin.

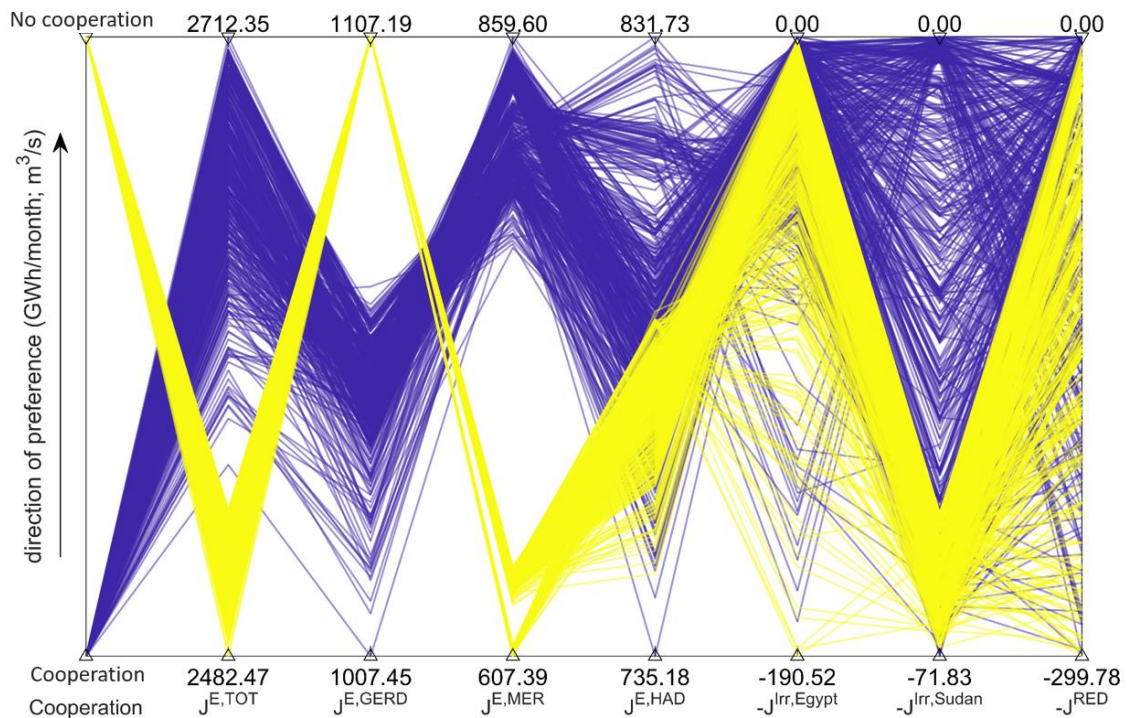


Figure 26 – Optimization of the Water Supply model under climate change for cooperative scenario (blue lines) and non-cooperative scenario (yellow line). For every solution is reported the hydropower production at the basin scale ($J^{E,TOT}$), in Ethiopia ($J^{E,GERD}$), Sudan ($J^{E,MER}$) and Egypt ($J^{E,HAD}$), Egypt irrigation deficit ($-J^{Irr,Egypt}$), Sudan irrigation deficit ($-J^{Irr,Sudan}$) and water reductions below HAD ($-J^{RED}$).

6. CONCLUDING REMARKS

In this Deliverable we explored the trade-offs and synergies emerging from the multi-objective design of portfolios integrating water supply and demand interventions in the NRB. We carried out several experiments considering historical and future scenarios of water availability and demand, as well as cooperation and non-cooperation scenarios between Ethiopia, Sudan and Egypt.

The analysis revealed the presence of a strong trade-off between the Sudanese agricultural sector and hydropower production at the basin scale, as water consumption for irrigation impedes hydropower production in the two dams downstream of the system (MER and HAD). On the other hand, there is no evidence of conflict between hydropower production and the Egyptian irrigation sector, as the latter is downstream of the system and does not subtract water from the hydropower plants. Although Sudan's consumption of water for irrigation may decrease the availability of water to meet Egyptian demand, the introduction of Egyptian water demand measures can alleviate the trade-off between these two sectors. Similarly, the introduction of water demand measures is able to mitigate the conflict between the Sudanese irrigation sector and hydropower production, reducing the water demand downstream benefits the upstream sectors. The optimization of the model with future scenarios showed how climate change will exacerbate the main trade-off between the hydropower and irrigation sectors, making even more essential the introduction of water demand reduction measures. In addition, GERD's hydropower production is projected to decline in future

scenarios due to a decrease in water availability in the Blue Nile. The simulation with cooperative scenarios showed that coordinating the operation of the three dams could bring significant benefits to the downstream countries, while their uncoordinated operation would only benefit Ethiopia and cause great damage to both the hydropower and irrigation sectors of Sudan and Egypt. Moreover, the decrease in water availability due to climate change makes more evident the necessity for these three countries to coordinate the management of their water resources.

Since reducing the water demand in Egypt is a crucial step for addressing the Water-Energy-Food-Ecosystem Nexus at the river basin (meso level) scale, we analysed how to integrate water reuse, groundwater, aquaponics and desalination in the Water Demand model. This analysis produced a large set of solutions that efficiently combine these four measures to reduce costs and negative environmental impacts. Results suggest that the most efficient way to allocate these measures is to place groundwater along the Nile Valley, outside the Delta, to reduce the risks of saline intrusion, and to construct desalination plants or rely on water reuse in the Delta. The more ambitious the water demand reduction target, the more it is necessary to use a combination of these measures and it is not possible to rely on just one. Yet, a high exploitation of groundwater or water reuse could lead to severe environmental impacts and degradation of water quality. A wide implementation of aquaponics and desalination requires instead very high costs, and may not be completely feasible given the current technological limitations of the two measures.

The use of this framework allows policy makers to test certain policies and compare them with the Pareto-efficient solutions identified by the optimisation. In addition, it also offers the possibility to optimise the whole system in case one wants to rethink current water management policies and strategies. The availability of a large number of excellent policies (so-called optimal solutions) offer a higher freedom to decision makers in identifying a policy they deem appropriate, while advanced solution visualisation systems, such as the parallel plots, make it easy and intuitive to navigate the space of alternatives. Including different scenarios allows to strategically plan effective policies for current water availability and to test such policies for future scenarios of climate change and population growth. In conclusion, our results show how it is possible to find alternative portfolios able to satisfy most of the stakeholders' interests. This is made possible by a coordinated management of the system's water infrastructures, combined with the introduction of innovative measures to reduce water demands in the Nile Valley and Delta. While in this report we focus on a single, nominal future scenario, in the next deliverable (D4.4) the robustness of the selected WEF planning portfolios will be tested under a wide range of uncertain future scenarios. State-of-the-art scenario discovery will be used for identifying critical future conditions (either hydroclimatic or socio-technological) under which a candidate portfolio becomes vulnerable to failure, based on different level of risk/regret.

7. REFERENCES

- Taye, M. T., Willems, P., & Block, P. "Implications of climate change on hydrological extremes in the Blue Nile basin: A review." *Journal of Hydrology: Regional Studies*, 2015: 280–29.
- Sutcliffe, J., & Brown, E. «Water losses from the Sudd.» <https://www.tandfonline.com/doi/abs/10.1080/02626667.2018603>, 2018: 527–541.
- Atlas, Nile Basin Water Resources. <https://atlas.nilebasin.org/>. 2016.
- Howell, P., & Allan, J. «The Nile: Sharing a Scarce Resource. An historical and Technical Review of Water Management and of Economical and Legal Issues.» *Cambridge University Press*, 1994.
- Elsayed, H., Djordjevic, S., Savic, D. A., Tsoukalas, I., & Makropoulos, C. «The Nile Water-Food-Energy Nexus under Uncertainty: Impacts of the Grand Ethiopian Renaissance Dam.» *Journal of Water Resources Planning and Management* 11 (2020): 146.
- Wheeler, K. G., Jeuland, M., Hall, J. W., Zagana, E., & Whittington, D. «Understanding and managing new risks on the Nile with the Grand Ethiopian Renaissance Dam.» *Nature Communications*, 2020.
- Multsch, S., Elshamy, M. E., Batarseh, S., Seid, A. H., Frede, H. G., & Breuer, L. «Improving irrigation efficiency will be insufficient to meet future water demand in the Nile Basin.» *Journal of Hydrology: Regional Studies*, 2017: 315–330.
- Nikiel, C. A., & Eltahir, E. A. «Past and future trends of Egypt’s water consumption and its sources.» *Nature Communications* 2021, 2021.
- Verhagen, J., van der Zaag, P., & Abraham, E. «Operational planning of WEF infrastructure: quantifying the value of information sharing and cooperation in the Eastern Nile basin.» *Environmental Research Letters*, 2021.
- Adriansen, H. K. «Land reclamation in egypt: A study of life in the new lands.» *Geoforum*, 2009: 664–674.
- statistics, Arab Republic of Egypt Central Agency for public mobilisation and. *Statistical Yearbook (Tech. Rep.)*. 2017.
- Arab Republic of Egypt, Ministry of Water Resources and Irrigation. *National water resource plan (nwrp) - water security for all (2017 - 2030 - 2037), egypt (Tech. Rep.)*. <https://openknowledge.worldbank.org/handle/10986/8320>, 2017.
- Maier, H. R. et al. «Evolutionary algorithms and other metaheuristics in water resources: Current status, research challenges and future directions. .» (Environmental Modelling & Software), n. 271–299 (2014).
- Giuliani, M. et al. «Curses, Tradeoffs, and Scalable Management: Advancing Evolutionary Multiobjective Direct Policy Search to Improve Water Reservoir Operations.» (J Water Resour Plan Manag), n. 142 (2015).
- Hadka, D. & Reed, P. Borg. «An Auto-Adaptive Many-Objective Evolutionary Computing Framework.» (Evol Comput) 21, n. 231–259 (2013).
- Bușoniu, L., Ernst, D., De Schutter, B. & Babuška, R. «Cross-entropy optimization of control policies with adaptive basis functions.» (IEEE Transactions on Systems, Man, and Cybernetics, Part B: Cybernetics) 41, n. 196–209 (2011).

- Giuliani, M., Lamontagne, J. R., Reed, P. M. & Castelletti, A. « A State-of-the-Art Review of Optimal Reservoir Control for Managing Conflicting Demands in a Changing World. .» (Water Resour Res) 2021.
- Giuliani, M., Quinn, J. D., Herman, J. D., Castelletti, A. & Reed, P. M. «Scalable Multiobjective Control for Large-Scale Water Resources Systems under Uncertainty.» (IEEE Transactions on Control Systems Technology) 1492–1499 (2018).
- Giuliani, M., Herman, J. D., Castelletti, A. & Reed, P. «Many-objective reservoir policy identification and refinement to reduce policy inertia and myopia in water management.» (Water Resour Res) 2014.
- Zatarain Salazar, J., Reed, P. M., Herman, J. D., Giuliani, M. & Castelletti, A. « A diagnostic assessment of evolutionary algorithms for multi-objective surface water reservoir control. .» (Adv Water Resour) 172–185 (2016).
- Pachauri, R. K. et al. «Climate Change 2014: Synthesis Report. Contribution of Working Groups I, II and III to the Fifth Assessment Report of the Intergovernmental Panel on Climate Change. .» (EPIC3Geneva, Switzerland, IPCC) s.d.
- Masson-Delmotte, V. et al. «Working Group I Contribution to the Sixth Assessment Report of the Intergovernmental Panel on Climate Change .» (Edited by. doi:10.1017/9781009157896.) 2021.
- Chiarelli, D. D. et al. « The green and blue crop water requirement WATNEEDS model and its global gridded outputs. .» (Scientific Data 2020 7:1 7, 1–9) 2020.
- Repository, ENTRO Knowledge. «Welcome to Eastern Nile Technical Regional Office (EN-TRO). .» (<http://entro.nilebasin.org/information-hub/entro-knowledge-repository>.) s.d.
- Bergström, S. & Rapporteur, S. « Development and application of a conceptual runoff model for Scandinavian catchments.» 1976.
- Bergström, S. «The HBV model. Computer models of watershed hydrology. .» 443–476 (1995).
- Barbara, Climate Hazards Center UC Santa. «Data Sets.» (<https://www.chc.ucsb.edu/data>.) s.d.
- Sandoval-Solis, S., McKinney, D. C. & Loucks, D. P. «Sustainability index for water resources planning and management.» (J Water Resour Plan Manag 137, 381–390) 2011.
- UNECE. «Reporting on SDG indicator 6.5.2 and under the Water Convention.» (https://unece.org/environmental-policy/water/transboundary_water_cooperation_reporting) s.d.
- Ševčíková, H. & Raftery, A. E. «bayesPop: Probabilistic Population Projections.» (J Stat Softw 75,) 2016.
- «Indicator | SDG 6 Data.» (<https://sdg6data.org/indicator/6.5.2>.) s.d.